Palaeogeography, Palaeoclimatology, Palaeoecology 497 (2018) 139–156

Contents lists available at ScienceDirect

Palaeogeography, Palaeoclimatology, Palaeoecology

journal homepage: www.elsevier.com/locate/palaeo

Low-latitude vegetation and climate dynamics at the Paleocene-Eocene transition – A study based on multiple proxies from the Jathang section in northeastern India

V. Prasad[a,*], T. Utescher[b,c], A. Sharma[a], I.B. Singh[d], R. Garg[a], B. Gogoi[e], J. Srivastava[a], P.R. Uddandam[a], M.M. Joachimski[f]

[a] BirbalSahni Institute of Palaeosciences, Lucknow 226007, India
[b] Senckenberg Research Institute, Frankfurt am Main, Germany
[c] Steinmann Institute, Bonn University, Nussallee 8, 53115 Bonn, Germany
[d] 17-11-2C Metro City Nishat Ganj, Lucknow 226007, India
[e] Department of Geological Science, Gauhati University, Guwahati, India
[f] Institut für Geologie und Mineralogie, Schlossgarten, 91054, Erlangen, Germany

ARTICLE INFO

Keywords:
Paleotropics
PETM
Precipitation
Palynology
Climate change
Rainforest

ABSTRACT

We present a multi-proxy study of an upper Paleocene-lower Eocene succession from the paleo-equatorial region. The study is carried out on a coal-bearing, shallow-marine succession exposed at Jathang, east Khasi hills, Meghalaya, northeastern India. The succession was deposited in a low-energy, coastal marsh-bay complex. Dinoflagellate cyst biostratigraphy yields a late Paleocene to early Eocene age for the section. The deposits of the lower part of the succession represent a transgressive systems tract (TST) defined by seven parasequences, each starting with bay sediments deposited during transgression, followed by a shallowing-upward bay fill-marsh deposit. In the vertical succession, each parasequence acquires an increasingly marine character, culminating in a maximum flooding surface at the Paleocene-Eocene boundary. It is followed by four shallowing upward parasequences deposited in a highstand systems tract (HST). Enhanced chemical weathering and high terrestrial supply are testified by raised SiO_2 and Al_2O_3 contents and high percentages of terrestrial palynomorphs. The pollen flora recovered from the Jathang section was used for quantitative paleoclimate and vegetation reconstructions. The Coexistence Approach was applied based on Nearest Living Relatives (NLRs) of sixty fossil species recorded at different stratigraphic levels. Seven climate variables were determined for the fossil assemblages, and, as a measure of the seasonality of climate, the number of dry months was estimated. Our study shows that during the Paleocene there existed warm, seasonally dry tropical climate conditions with mean annual temperature at ca. 24–26 °C and mean annual precipitation at ca. 700–1800 mm, and with a dry season of 5–6 months. Particularly warm and wet, perhumid climate conditions with 26–27 °C and 2200–3200 mm mean annual precipitation with a dry period of 2–3 months were reconstructed for the latest Paleocene-earliest Eocene interval. The study shows a distinct vegetational turnover from palm-dominated, seasonally dry tropical forest during the Paleocene to highly diversified dicotyledonous megathermal rainforest during the latest Paleocene-early Eocene. The present study demonstrates that the reduced duration of the dry period during the latest Paleocene-earliest Eocene, due to a more active hydrological cycle, played a major role in determining the climate and shaping the vegetation cover in the paleo-equatorial region. There is evidence from our data that seasonality of rainfall is the determining factor for the tropical forest vegetation pattern of the equatorial region rather than mean annual rainfall condition. As the main trigger for the observed step-wise changes of the hydrology along the studied succession, the fast northward movement of the Indian Plate is inferred.

1. Introduction

The currently observed trend of increasing average mean surface temperature is a well-documented phenomenon and continues to occupy a central position in discussions on environmental issues. The last 150 years have seen a rise in atmospheric CO_2 concentration from 280

* Corresponding author.
E-mail address: prasad.van@gmail.com (V. Prasad).

https://doi.org/10.1016/j.palaeo.2018.02.013
Received 22 September 2015; Received in revised form 9 February 2018; Accepted 10 February 2018
Available online 19 February 2018
0031-0182/

to 400 ppm and an increase in ambient temperature (IPCC, 2007). Current trends indicate that this rise in both CO_2 and temperature is expected to continue, attaining levels that will, without any doubt, affect both flora and fauna, including mankind. There have been efforts to detect analogues that may expose the long-term effect of global warming on the bio-geosphere and to enable a more precise prediction of future climate. These attempts however, have been hampered by the absence of such analogues from the recent past. Climate model scenarios based on numerical simulations related to a significant increase in CO_2 level expected for the not so distant future are difficult to validate using data from the recent past. The early Paleogene greenhouse climate in deep time geological records offers an understanding of a longer-term effect of raised CO_2 on ecosystems. The Paleocene-Eocene Thermal Maximum (PETM), a well-studied extreme, globally warm event, followed by several small scale hyperthermal events, provides an important context within which to study temperature and precipitation data for a globally warm climate state.

Obtaining quantitative paleoclimate estimates for the early Paleogene greenhouse climate is one of the most crucial aspects of paleoclimate research during the last few decades. In contrast to the unambiguous records of the high temperature state of polar and high latitudinal regions during the Paleocene-Eocene interval, divergent hypotheses have been suggested for the climate at low latitudes (D'Hondt and Arthur, 1996; Huber, 2008). Past changes in the hydrological regime i.e. precipitation/evaporation, that mainly determine the continental climate in tropical regions, are a challenging issue. Quantitative data based on continental, paleobotanical proxies involving precipitation and its seasonal patterns are scarce (Anupama et al., 2000; Barboni et al., 2003; Vincens et al., 2007). Model simulations of future warming generally suggest warming mainly at higher latitudes (Masson-Delmotte et al., 2006; Cohen et al., 2014). However, there are discrepancies in terms of tropical precipitation changes (Allen and Ingram, 2002; Clark, 2004; Meehl et al., 2000; Williams et al., 2015). While the radiative forcing induced by the increase of greenhouse gases is spatially relatively uniform, tropical precipitation exhibits large variations between simulations, producing both positive and negative rainfall anomalies (Chou and Neelin, 2004; Chou et al., 2008). In order to better validate simulations of precipitation patterns in the tropical region anticipated for future climate scenarios, well-resolved quantitative precipitation data for the Paleocene-Eocene intervals from multiple tropical locations are required.

During the late Paleocene - early Eocene, the northern part of the Indian Plate occupied a near-equatorial position (Scotese and Golanka, 1992; Sluijs et al., 2008). This period also witnessed marine transgression along the coastal zone of India, initiating carbonate sedimentation. A humid climate during the late Paleocene to earliest Eocene led to the development of peat swamps in the coastal areas of the northeastern and western margins of the Indian subcontinent (Prasad et al., 2013). In the northeastern region of India, in the Garo-Khasi-Jaintia Hills, the Paleocene-Eocene sedimentary successions consist of thin pinching and discontinuous but workable coal seams. The rich plant fossils present in this coal offered a unique opportunity to investigate floral and faunal changes during the Paleocene-Eocene transition in a tropical setting. Coal and lignite bearing deposits of the Indian subcontinent have yielded a large number of pollen, megaflora, insects, marine fishes and a variety of mammalian fossils (Dutta and Sah, 1970; Kar and Kumar, 1986; Samant and Phadtre, 1997; Tripathi et al., 2000; Sahni et al., 2004; Bhandari et al., 2005; Prasad et al., 2006; Sahni et al., 2006; Rose et al., 2006; Garg et al., 2008; Prasad et al., 2009; Clementz et al., 2010; Prasad et al., 2013; Shukla et al., 2014; Srivastava and Prasad, 2015; Kumar et al., 2016). Most of the late Paleocene-early Eocene successions of northeastern India represent coastal to shallow marine deposits. The Jathang section in northeastern India is a coastal deposit of late Paleocene-early Eocene age and is thought to include the pre and post PETM events (Prasad et al., 2006). The basic stratigraphy and sedimentological analysis of the Jathang section were presented in Prasad et al. (2006). In the present study, the section is further interpreted in terms of parasequences and systems tract analysis in response to sea level changes to provide a depositional framework. The geochemical analysis was carried out to understand the intensity of weathering in the provenance area during the Paleocene-Eocene. A Carbon isotopic study was carried out in order to identify major shifts in the $\delta^{13}C$ values. Being coastal marine in nature, the Jathang section has both marine and terrestrial biotic components. This provides us with an opportunity to investigate changes in the terrestrial plant communities in relation to changes in the CO_2 concentration, temperature and precipitation.

Nearest Living Relatives (NLRs) of most of the early Paleogene fossils are already known (Prasad et al., 2009). Based on the assumption that Cenozoic plant taxa have similar climatic requirements to their NLRs, the Coexistence Approach (CA) was applied on the recovered fossil pollen flora from Jathang, East Khasi Hills, Meghalaya, northeastern India to obtain a quantitative climate reconstruction across the Paleocene-Eocene transition from a paleo-equatorial region.

In detail, the following questions are addressed: How was tropical plant diversity of the paleo-equatorial belt affected by markedly warm climates during the late Paleocene and early Eocene? How did temperature and precipitation evolve throughout the late Paleocene and early Eocene in a paleo-equatorial region? How did the ecosystem respond to climate changes across the Paleocene-Eocene transition?

2. Geological setting, stratigraphy and sedimentology

The separation of the Indian landmass from Gondwanaland, its movement from southern high latitude across the equator to the subtropical zone of the Northern Hemisphere, and its final collision with Asia (at 50 Ma ± 10 Ma) resulted in large-scale continental plate reorganization. The Assam-Arakan Basin in India was initiated during the late Campanian with sedimentation starting in the southern part of the Meghalaya region (Garg et al., 2006; Singh and Swamy, 2006). The southern fringes of the Shillong Plateau, collectively known as South Shillong Plateau, comprise the Garo-Khasi-Jaintia hilly tract in Meghalaya (Fig. 1). Sedimentation started with coarse-grained clastics at the base, known as Mahadeo Formation (Campanian-Maastrichtian), in a rift-related coastal setting, later on converting into prominent carbonate platform condition represented by the Sylhet Limestone Formation. The Sylhet Limestone Formation, consisting of three horizons of fossiliferous limestone interposed by two bands of sandstone, witnessed several phases of sea-level fluctuations during the depositional history of the Shillong Plateau (Raja Rao, 1981; Wilson and Metre, 1953). All the three limestone units contain datable larger benthic foraminifera in association with calcareous algae (Jauhri and Agarwal, 2001; Nagappa, 1959; Wilson and Metre, 1953). In the Jathang Hill of the Mawsynram area, only the lower most Lakadong Limestone Member and Lakadong Sandstone Member are present (Table 1). Both members occur as small outcrops and commonly occupy the top of the hillocks in the area (Figs. 1, 2). The section is 26 m thick, consisting of 3.5 m light grey to dark grey coloured hard and compact limestone of the Lakadong Limestone Member at the base containing larger benthic foraminifera and calcareous algae, while the 20.5 m thick overlying Lakadong Sandstone Member is the uppermost lithological unit in the study area (Figs. 1, 2). The Lakadong Sandstone Member of Jathang comprises a succession of mudstone, sandstone, carbonaceous shale, and coal (Fig. 2). Three lithofacies were identified which are cyclically repeated.

Mudstones make up 10–20 cm thick horizons. Essentially they represent clayey siltstones within sand layers. They display millimetre-scale alternations of sand and silt layers, sometimes with small ripple bedding pointing to deposition in a shallow bay under low-energy conditions.

Sandstones make up 50 cm to 2 m thick horizons. They exhibit low-angle crossbedding, parallel bedding, and bands of rippled layers. Thick

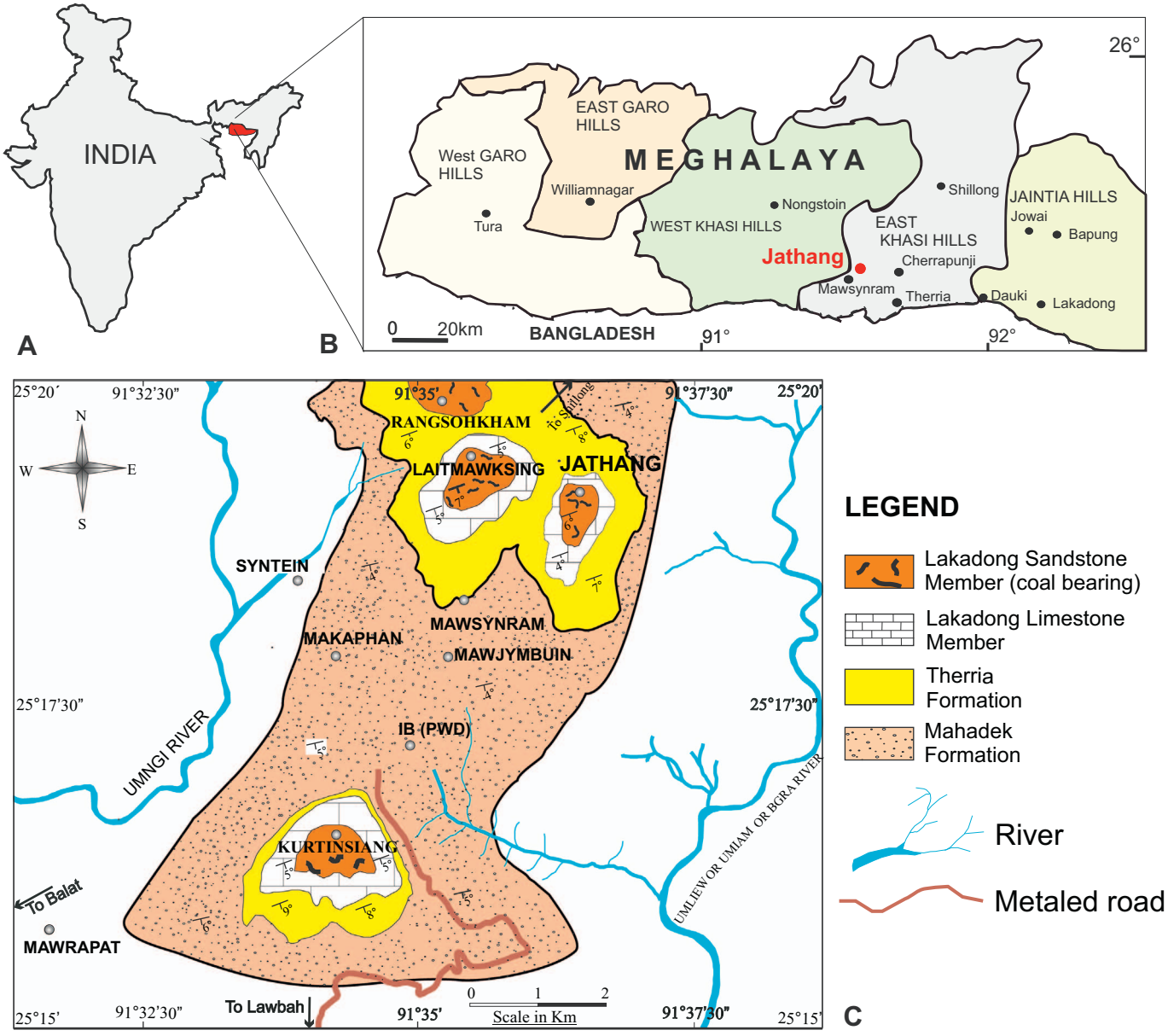

Fig. 1. Location of the study area (A and B) and geological map over the area of Jathang Hill (C). (After Gogoi et al., 2009).

sandstones may be amalgamated units representing deposits of sandy shoals and coastal sand barriers.

Carbonaceous shales and coals consist of few decimetre-thick coal bands associated with millimetre to centimetre-thick sand layers alternating with dark mud layers. This lithofacies represents deposits of a coastal marsh.

The different lithofacies show cyclic arrangements in distinct parasequences. Each parasequence is made up of three lithofacies i.e., mudstone-sandstone-coal representing a shallowing upward succession (Fig. 3). In the Jathang section, eleven parasequences are identified. The lower seven parasequences represent deposits in a transgressive systems tract (TST) with gradually rising sea-level and increasing marine influence (Fig. 3). On top of parasequence seven, the maximum flooding surface (MFS) is identified showing high abundance and diversity of dinoflagellate cysts indicating a maximum marine influence. The MFS is characterized by the increased proportion of dinoflagellate cysts including a numerical abundance of *Apectodinium* dinoflagellate cysts along with other gonyalocoid dinocyst forms. This part of the sequence may include the PETM event (Prasad et al., 2006). The deposits above the MFS show four shallowing upward parasequences deposited in a highstand systems tract (HST) (Fig. 3).

2.1. Age of the Jathang succession

The clastics-dominated facies of the Late Paleocene-early Eocene at Jathang does not permit plankton-based zonation and correlation as calcareous microfossils (foraminifera and nanofossils) are completely missing. A biostratigraphic framework based on dinoflagellate cysts has been established for the Jathang section (Prasad et al., 2006) (Fig. 4). Samples JTS1–JTS7 contain few poorly preserved dinoflagellate cysts along with foraminiferal test linings only. The presence of diverse dinoflagellate cyst assemblages from JTS 15 onwards allows the

Table 1
Lithostratigraphic setup of the Paleogene succession of Khasi hills.
(Modified after Raja Rao, 1981; Garg and Khowaja-Ateequzzaman, 2000; Prasad et al., 2006).

STAGE	AGE	FORMATION/ MEMBER		LITHOLOGY
EOCENE	YPRESIAN	SYLHET LIMESTONE FORMATION	UMLATDOH Lst	Grey to pinkish grey foraminiferal limestone with calcareous sandstone partings
PALAEOCENE	THANETIAN		LAKADONG Sst	Predominantly buff to whitish, soft friable, medium to coarse grained arkosic sandstone, often pyriteous frequently burrowed, carbonaceous shales and siltstones and thin coal seams
			LAKADONG Lst	Grey to brownish grey foraminiferal-algal limestone, dolomitic at the base with thin grey shale, silty shale partings
	SELANDIAN	THERRIA FORMATION		Hard buff to brownish, medium to coarse, ferrugenous sandstone with thin bands of pyriteous siltstone and carbonaceous shale

dinoflagellate biostratigraphic zonation scheme to be applied in the stratigraphic succession. The assemblage consists of rich Wetzelielloids dinoflagellate forms involving *A. homomorphum* and *A. quinqueleatum* and moderate occurrences of *A. paniculatum*, and *Apectodinium* cf. *augustum*, now *Axiodinium augustum* (Williams et al., 2015) in JTS 16-JTS 18 (Figs. 4, 5). > 200 counts of *Apectodinium* species characterized by high abundance of *A. homomorphum* and *A. quinqueleatum* and moderate occurrences of *A. hyperacanthum*, *A. paniculatum* and few *Axiodinium* cf. *augustum* (Figs. 5, 6) were defined as *Apectodinium* acme horizon in samples JTS16-JTS18. The *Apectodinium* acme is a unique feature that characterizes the Late Paleocene-early Eocene marine successions of low, mid and high latitudinal regions. However, the presence of an *Apectodinium* acme should not be taken as a criterion to define the Paleocene-Eocene boundary, particularly in low latitudes where *Apectodinium* abundances were reported prior to the P-E boundary (Bujak and Brinkhuis, 1998). However, it has been considered that *Axiodinium augustum* has a very narrow range that appeared slightly before or at the beginning of the PETM, at the onset of the Carbonate Isotope Excursion (CIE) (Bujak and Brinkhuis, 1998; Crouch et al., 2001; Crouch et al., 2003; Egger et al., 2003; Harding et al., 2011; Kender et al., 2012; Eldrett et al., 2014; Iakovleva, 2016) in JTS 17 (Figs. 4, 5). The first appearance of *Axiodinium* cf. *augustum* in sample JTS 17, along with dominance of *A. homomorphum* and *A. quinqueleatum*, and moderate number of *A. Hyperacanthum* and *A. paniculatum* (Figs. 4–6), defines the base of the Aau biozone of Powell (1992) and dinoflagellate cyst sub-biozone D5a of Costa and Manum (1988). Hence, the *Apectodinium* acme consisting of *A. augustum* at JTS 17 probably defines the Paleocene-Eocene boundary. The numerical abundance of several wetzelielloid dinoflagellate cysts (sample JTS 22-JTS 30) shows similarity with the recently reported wetzelielloid dinoflagellate species from the basal Eocene successions of northern Kazakhstan (Iakovleva, 2016). *Epelidinium brinkhuisii*, *Vallodinium picardicum*, and *Stichodinium parisiense*, wetzelielloid dinoflagellate cysts present in the upper part of Jathang (Figs. 4, 7), are comparable to earliest Eocene assemblages of northern Kazakhstan (Iakovleva, 2016). These studies also point to a regional correlation between the Indian and northern Kazakhstan (former Turgay Strait) Paleocene to Eocene successions and may also indicate migration of tropical plankton in the Tethyan realm, as a result of globally warm climate conditions.

3. Materials and methods

3.1. Stratigraphic analysis

The Jathang section was measured using a measuring tape and Brunton Compass. The section was identified into distinct lithofacies using physical parameters i.e. grain size, physical sedimentary structures, and biogenic structures. The observed cyclicity of the lithofacies allows for identifying parasequences, in each case representing shallowing upward cycles (Fig. 3). Changes in the degree of marine influence within the parasequences are used to interpret the Systems Tract and sea-level changes.

3.2. Geochemistry

To carry out geochemical analysis, 26 samples (ca. 200 g) were initially homogenized, and a part of the same (ca. 50 g) was crushed to about −200 mesh size in an agate mortar. Sample powders were then oven dried (~100 °C for 12 h), and pressed pellets were prepared. The pellets thus prepared were analyzed for major elements using the wavelength dispersive XRF (WD-XRF) technique (Siemens SRS-3000) at WIHG, Dehradun. Details regarding the pellet preparation methodology are available elsewhere (e.g., Stork et al., 1987; Saini et al., 2000). The quality of the analysis (precision and accuracy) was checked using several international reference standards of soil and sediments, e.g., SO-1, GSS-1, GXR-6, SCO-1, SGR-1, SDO-1, MAG-1, GSD-9, GSR-6 and BCS-267. The accuracy of measurement is better than 2–5%. As a measure for the chemical maturity of the sediments we calculated the Chemical Index of Alteration (CIA) according to Nesbitt and Young (1984) using mole percentages of oxides [CIA = $Al_2O_3 / (Al_2O_3 + Na_2O + CaO^* + K_2O) \times 100$], with CaO* representing CaO of the silicate phase only.

3.3. Carbon isotopic analysis

Organic carbon isotopic analysis was carried out on 15 samples of the Lakadong Sandstone of the Jathang section. The organic carbon was extracted from 10 mg sediment in each case. Samples were washed with deionized water and then treated with 30% HCl to dissolve any carbonate. The residues were washed thoroughly with deionized water, dried and homogenized in a mortar. The analyses were performed with an elemental analyzer (CE 1110) connected on-line to a Thermo Finnigan Delta Plus mass spectrometer (at the University of Erlangen-Nuremberg, Germany). All values are reported in the standard δ notation in permill relative to V-PDB. Accuracy and reproducibility were monitored by replicate analysis of the graphite standard USGS 24–16.049‰. The reproducibility was better than ± 0.1‰ (1 std. dev.).

3.4. Pollen analysis

A total of 30 samples from the Jathang section were studied for palynological analysis. The samples were prepared following the standard palynological technique which includes treatment with 10% HCl, 40% HF to digest carbonates and silicates followed by mild oxidation with 10% HNO_3 to remove excess amorphous organic matter. In order to remove humic substances 1% KOH solution was also used, and lastly, the washed samples were sieved with a 10 μm mesh sieve. The residue was examined under the light microscope for organic content. Permanent slides were prepared by spreading evenly a drop of maceral with polyvinyl alcohol on glass cover slips. After drying, the coverslips were fixed on the glass slides using a mounting medium Canada balsam. We counted 200–350 pollen and spores using a DM 2500 Leica Microscope.

Species richness ($D = s/\sqrt{N}$ where D is the Menhinick's Index for species richness, s equals the number of taxa represented in one sample and N is the total number of specimens in one sample) along with

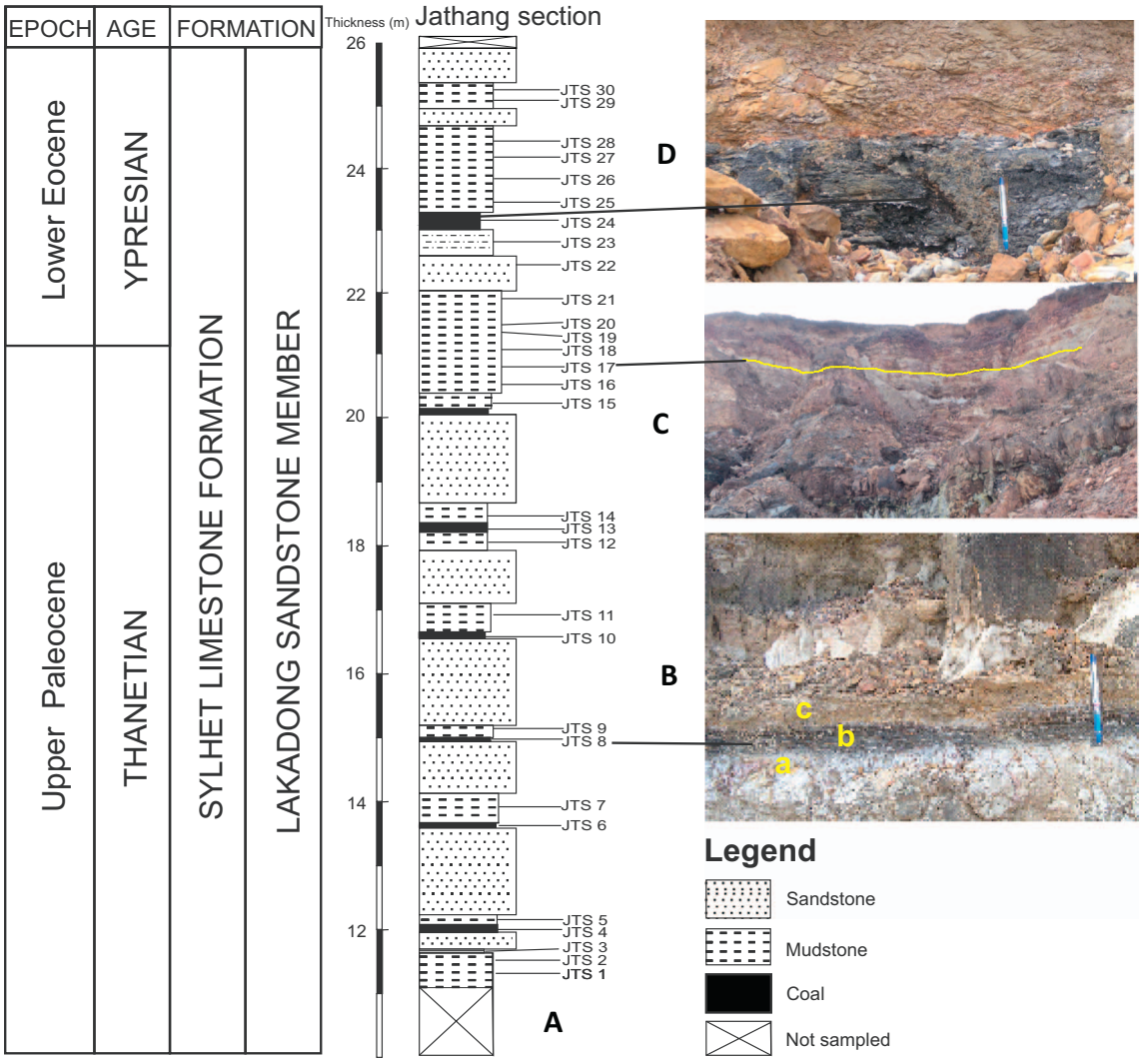

Fig. 2. Stratigraphic section at Jathang (A) showing various lithologies. B: Facies sequence showing sandstone (a), thin coal layer (b), and mudstone (c). C: Paleocene-Eocene boundary layer demarcated by yellowline in the stratigraphic succession. D: Coal layer and associated shales.

species standing diversity (taxonomic diversity of a group at the mid-point of a time interval; cf. Harper, 1975) was calculated to determine the palynofloral diversity pattern. Individual relationships between pollen species richness and climate variation i.e. mean annual temperature (°C), mean annual precipitation (mm), mean dry days, coldest month temperature (°C), warmest month temperature (°C), mean dry month precipitation (mm), mean wet month precipitation (mm) and mean warm month precipitation (mm) as well as number of dry months datasets were compared using linear regression analysis and correlation coefficients (r). Tests for normality (Shapiro-Wilk) and parametric statistics such as *t*-test were also used for hypotheses testing of distributions of species richness (D), standing diversity and correlation coefficient (r). All the statistical analyses were performed in Past 3.0 Paleontological Statistics Software (Hammer et al., 2001).

3.5. Palynological records

The coal bearing succession of Jathang exhibits highly diverse and rich assemblages of palynomorphs belonging to palms, coastal mangroves, lowland forest, and inland tropical rainforest. The dinoflagellate cysts at selected levels are indicative of a shallow marine depositional environment. Fossil pollen recorded from the section were assignable to the angiosperm families Arecaceae, Liliaceae, Bombacaceae, Euphorbiaceae, Clusiaceae, Proteaceae, Anancardiaceae, Barringtoniaceae, Caesalpiniaceae, Polygalaceae, Rubiaceae, Rhizophoraceae, Podocarpaceae, Araceae, Pedaliaceae, Sarcolaenaceae, and Dipterocarpaceae.

3.6. Coexistence approach

The terrestrial fossil pollen records were used for climate reconstruction by applying the Coexistence Approach (Mosbrugger and Utescher, 1997; Utescher et al., 2014). Information available from previous works (Thanikaimoni et al., 1984; Tissot et al., 1994; Prasad et al., 2009) has been used to supplement data on NLRs presented here. The distribution of the NLRs and their climatic requirements were determined at a global scale, using the latest version of the Paleoflora database (Utescher and Mosbrugger, 2014), as well as other literature resources. The fundamental idea of the Coexistence Approach assumes that the climatic requirements of fossil taxa are similar to those of their NLRs. Hence, mean annual temperature (MAT), mean temperature of the warmest month (WMT), mean temperature of the coldest month (CMT), mean annual precipitation (MAP), mean precipitation of the wettest month (MPwet), driest month (MPdry) and warmest month

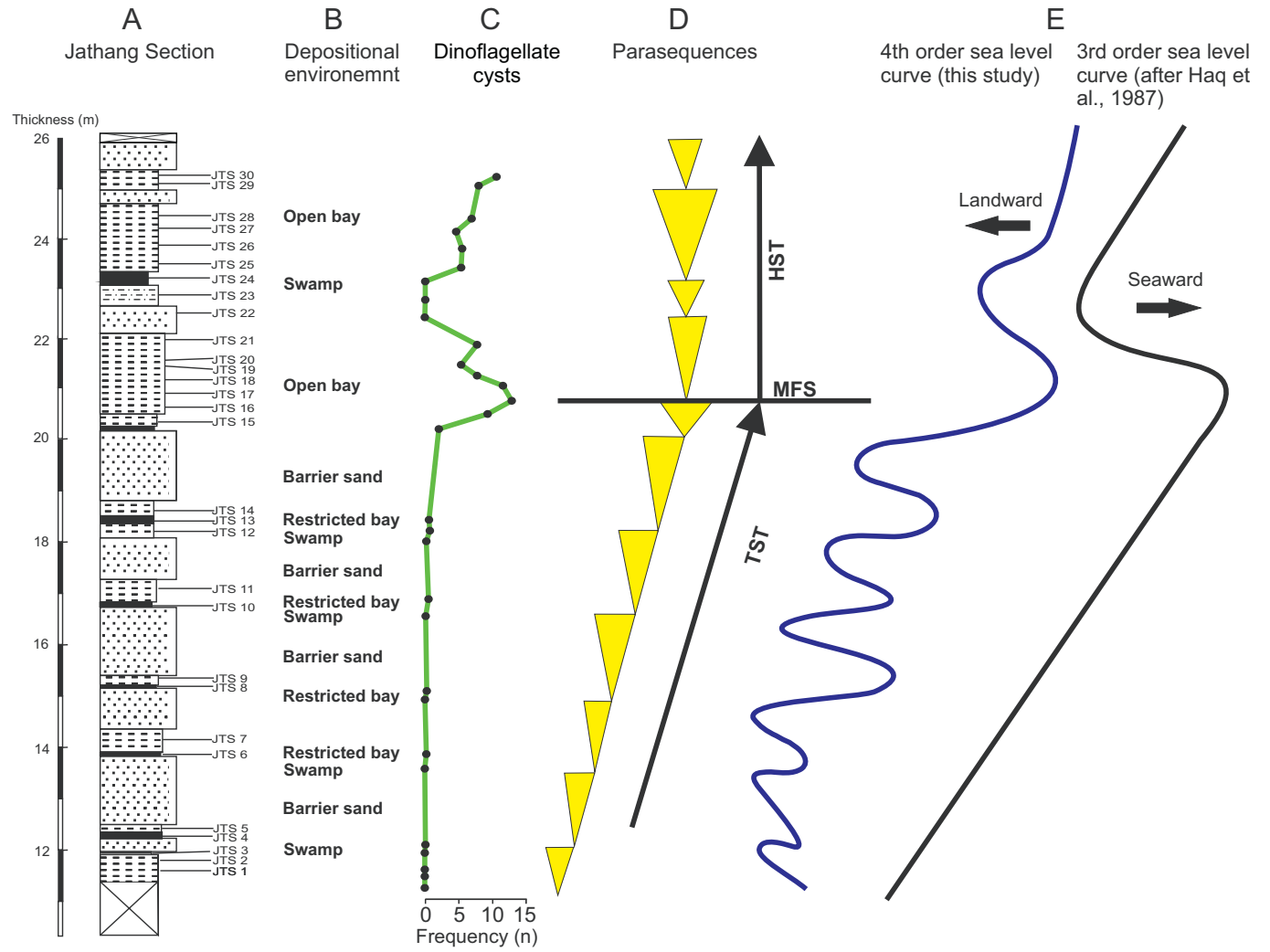

Fig. 3. Jathang succession (A), depositional environments (B), abundance of dinoflagellate cysts (C), parasequences (D), systems tracts (E), and sea-level curves (F). 4th-order sea-level curve from this study, 3rd-order sealevel curve after Haq et al. (1987).

(MPwarm) of the NLRs were determined. Moreover, the length of the dry season, tolerated by the NLRs in each case, was also taken into consideration and was determined for selected modern taxa. To reconstruct past climate, coexistence intervals were determined for each of the climatic parameters, separately for each stratigraphic level. Further, the coexistence intervals were plotted against the stratigraphic column. See supporting online table for the complete set of climate data reconstructed for Jathang including list of taxa used to estimate the length of the dry season.

3.7. Estimate of the length of the dry period

Rainfall seasonality is a dominant ecological factor in maintaining tropical diversity and vegetation composition in a tropical forest biome (Pascal and Pélissier, 1996; Barboni et al., 2003). The floristic composition in a tropical forest ecosystem varies according to the number of days without rainfall during the dry season (Barboni et al., 2003). Hence in the present study, the number of dry months/days was calculated for selected NLRs and plotted along with other climatic parameters against the stratigraphic column. Since most of our NLRs are today native to the southern Western Ghats area hence the required information was taken from published records of that region (Ramesh and Pascal, 1997) and from the Paleoflora database (Utescher and Mosbrugger, 2014).

4. Results

4.1. Carbon isotopes

Carbon isotope data of *Apectodinium* dominating the upper part of the Jathang section are provided in Prasad et al., 2006. In this study, the carbon isotope analysis for the complete Jathang section is presented (Fig. 8). The $\delta^{13}C$ values of the Jathang section range between −23.9‰ and −27.9‰ (Fig. 8). In the basal part, the $\delta^{13}C$ values of JTS 1and JTS 3 are −25‰. Sample JTS 6 shows a considerably negative value of −27.64‰, followed by a slightly less negative value of.

−25.9‰ for JTS 7 and 8 (Fig. 8). Sample JTS 9 again shows a negative value of −27.98‰ and a complimentary trend in JTS 11 (−23.9‰) while consistently negative values of −26.9‰ to.

−27.8‰ for JTS 16 - JTS 19 and relatively less negative values of −25.8‰ to −26.5‰ for JTS 20 - JTS 30 were determined (Fig. 8).

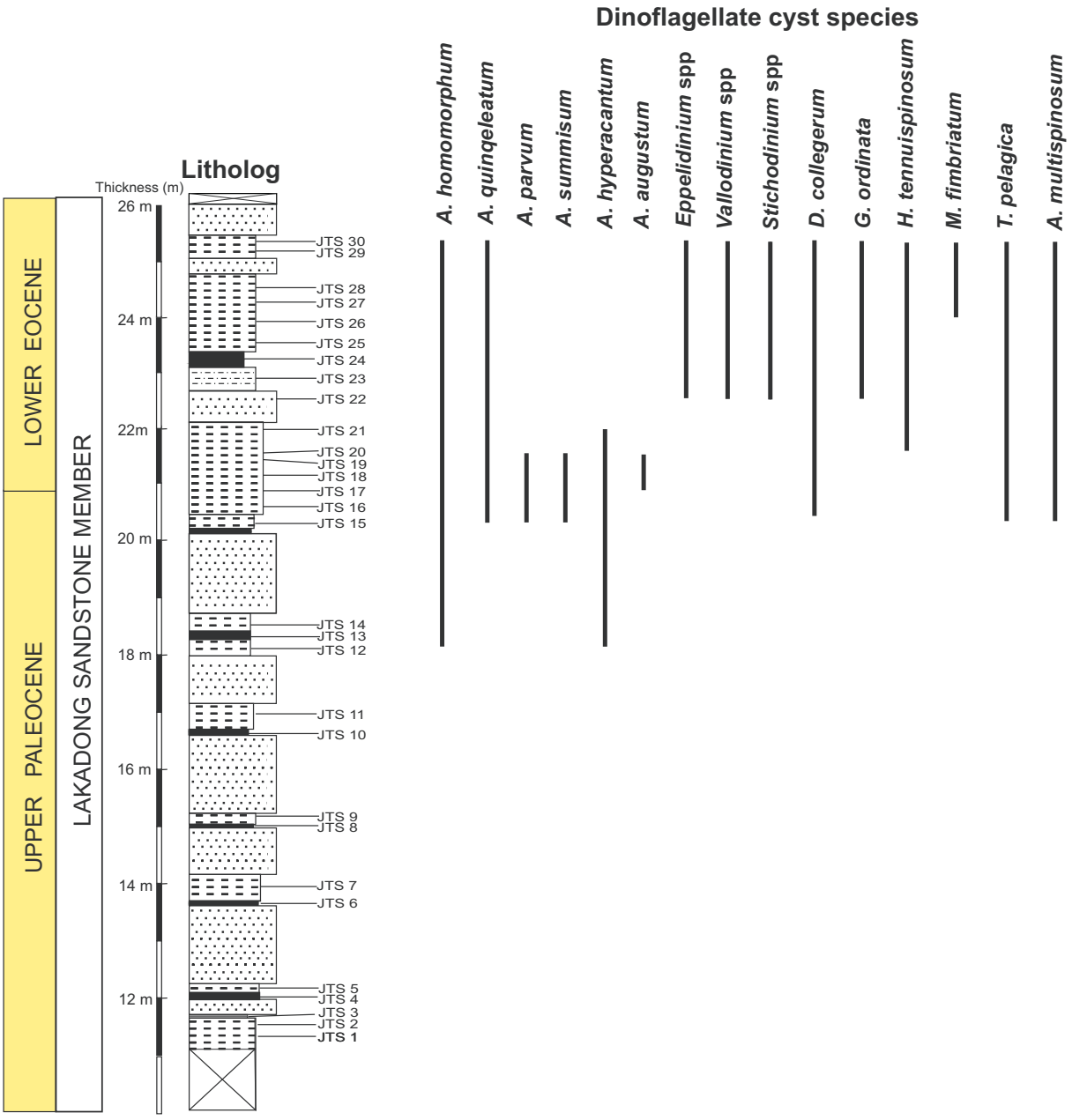

Fig. 4. Stratigraphic ranges of dinoflagellate cysts in the Jathang section.

4.2. Geochemistry

The geochemical data of major elements show a significant variation over the entire sedimentary succession. In order to better understand the variations in the elemental abundances, coal and sandstone samples were not considered for comparison because very high values for organic carbon and silica content respectively mask the changes in other elements, otherwise observed in the sequence. Therefore, texturally comparable sediments (shale/mudstone) were taken into consideration. The aluminium (Al_2O_3) and titanium (TiO_2) variation patterns show a complementary trend with the silicon (SiO_2) variation in the sequence (Fig. 9). The potassium (K_2O) variation pattern mostly follows the silica pattern (Fig. 9). The abundances of calcium (CaO), sodium (Na_2O), and magnesium (MgO), all highly mobile under surface conditions, are very insignificant indicating that these elements were flushed out during intense weathering in the catchment region. The variations noticed in iron (FeO) and manganese (MnO) are more or less similar and show increased abundance in samples associated with the coal horizons, due to favourable redox conditions at the depositional site. CIA values > 85 were obtained for all 26 samples analyzed while in the lower and middle part of the section very high CIA values of > 95 are attained.

4.3. Paleocene palynofloral assemblage

The palynomorphs recovered from the lower part of the section are *Arecipites bellus*, *Arecipites* sp., *Kelmeyerapollenites* spp., *Palmaepollenites eocenicus*, *Monocolpites* sp., *Matanamadheasulcites kuthchensis*, *Racemonocolpites* sp., *Liliacidites longicolpatus*, *Liliacidites* sp., *Proxaperties operculatus*, *Lakiapollis ovatus*, *Polylongicolporites retipilatus* (Fig. 10). The majority of the NLRs of the fossil pollen belong to a variety of palms of the Arecaceae family. However, *Kelmeyerapollenites* spp., shows affinity with the pollen of the living species *Perrierodendron boinense* of the Sarcolaenaceae family. The NLR of *Lakiapollis ovatus*

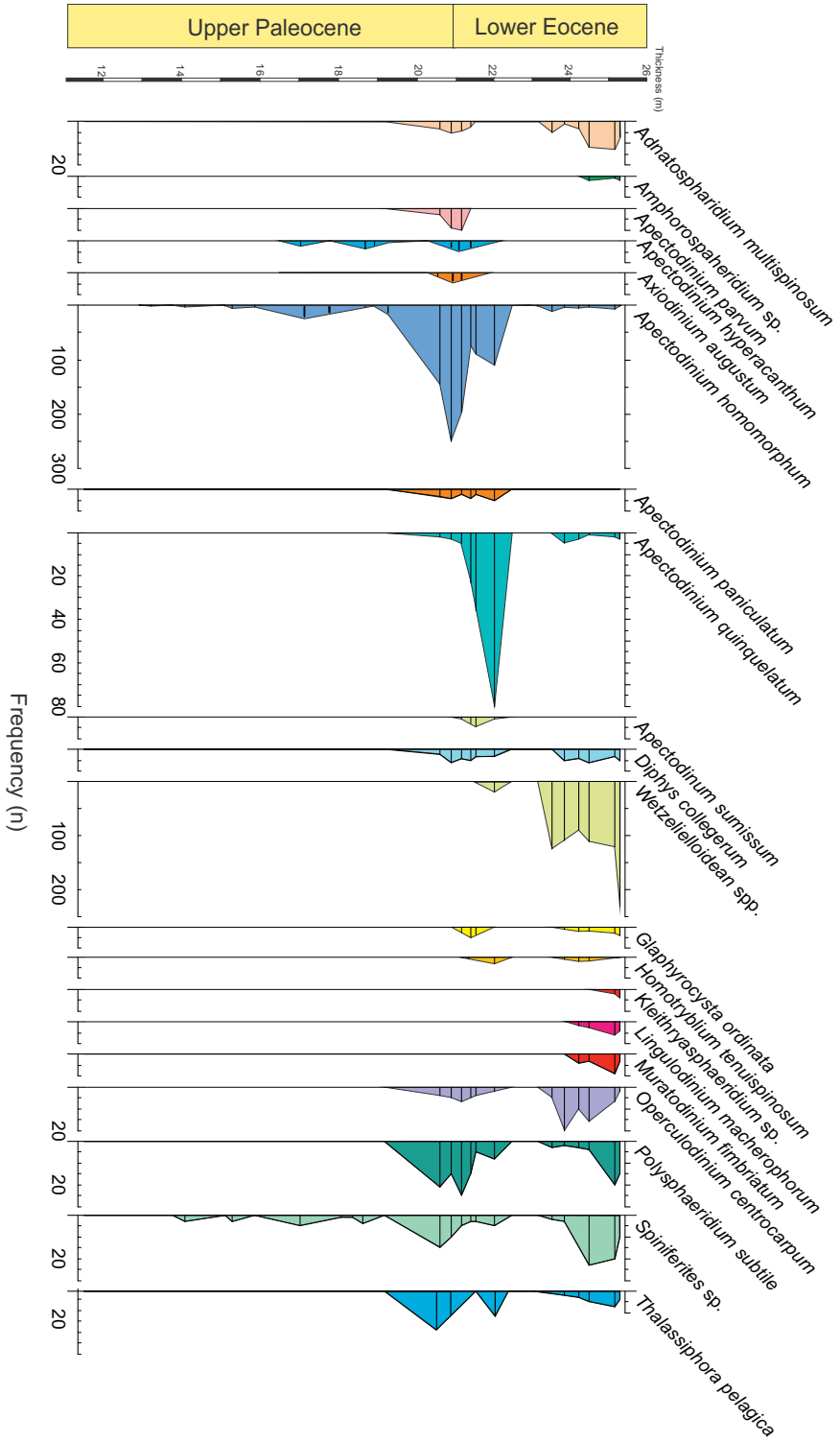

Fig. 5. Dinoflagellate cyst counts from the Jathang succession. Wetzelielloid spp. include *Epelidinium brinkhuisii*, *Vallodinium picardicum*, and *Stichodinium parisiense*.

belongs to *Durio* sp. of the Bombacaceae family while fossil *Polylongicolporites retipilatus* shows a striking resemblance to the pollen of the extant *Monotes kerstingii* of the Dipterocarpaceae family of Africa, and *Monocolpites* sp. with living genera of the Magnoliaceae family.

4.4. Palynofloral assemblage of the early Eocene

The palynofloral assemblage shows an increase of perhumid tropical forest elements in both abundance and diversity (Fig. 10). The recorded fossil palynomorphs are *Albertipollenites* sp., *Dipterocarpusretipilatus*, *Tricolpites reticulates*, *Polybrevicolpites indistinctus*, *Sastripollenites trilobatus*, *Retimonocolpites thanikaimoni*, *Tricolporocollumellites pilatus*, *Tricolporopollenites robustus*, *Retitribrevicolporites matanamadhensis*, *Paleocaesalpiniacipites eocenicus*, *Polygalacidites* sp., *Lanagiopollis subglobatus*, *Lanagiopollis* sp., *Lanagiopollis ruguloverrucatus*, *Lanagiopollis emarginatus*, *Rhoipites* sp., *Meliapollis inevelii*, *Proxapertites cursus*, *Proxapertites*

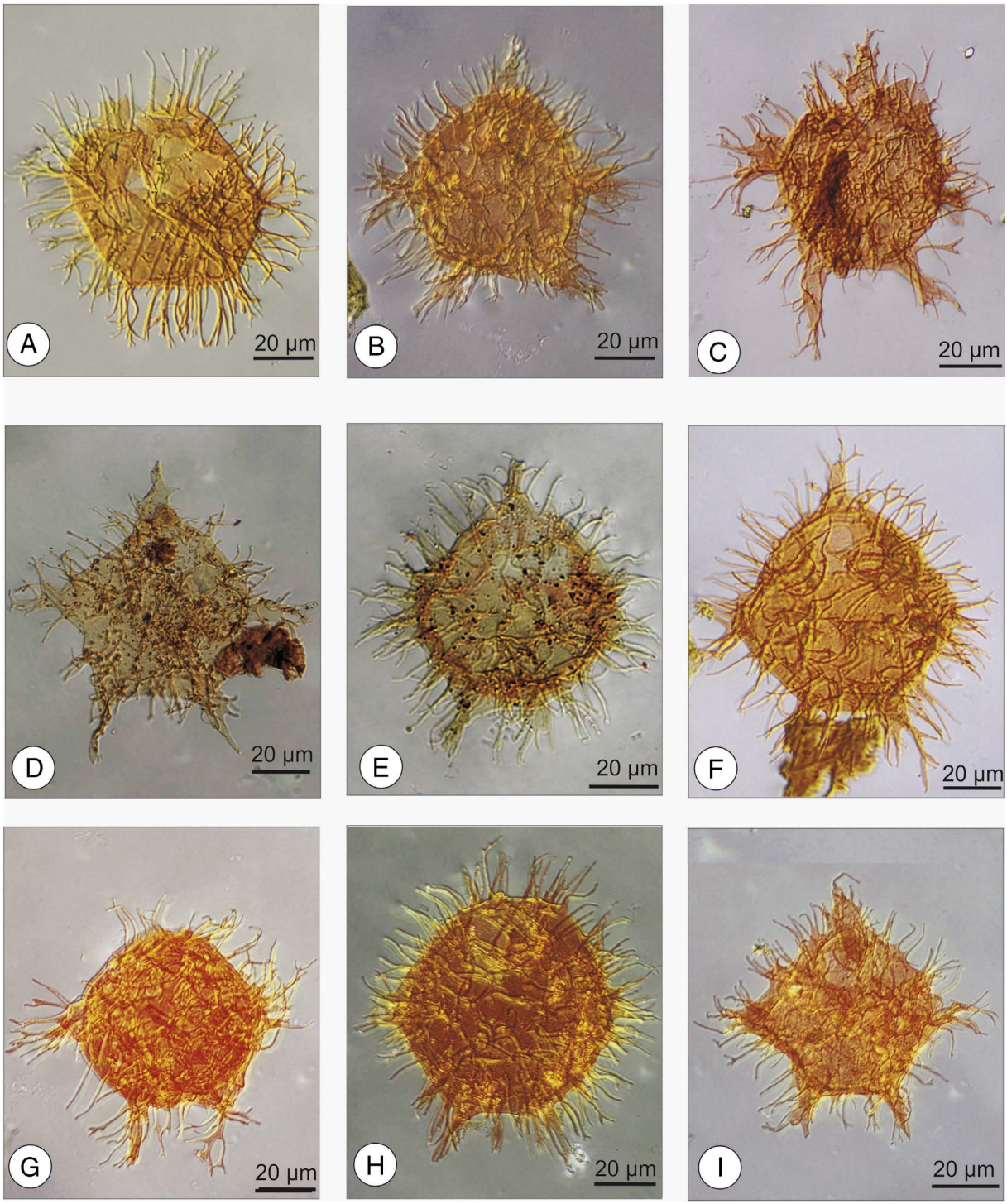

Fig. 6. Dinoflagellate cysts with slide numbers and England finder coordinates.
A, *Apectodinium homomorphum*, BSIP 14665, N 42-2; B, *Apectodinium paniculatum*, BSIP 14665, K 31-2; C, *Apectodinium hyperacanthum*, BSIP 14667, N 11-2; D, *Axiodinium augustum*, BSIP 14666, N 44-3; E, *Apectodinium quinquelatum*, BSIP 14665, U 26-2; F, *Apectodinium quninquelatum*, BSIP 14667, T 29-2; G, *Apectodinium hyperacanthum*, BSIP 14667, 17-4; H, *Apectodinium homomorphum* BSIP 14667, J 15-4; I, *Apectodinium paniculatum*, BSIP 14667, J 43-4.

assamicus, *Proxapertites crassimurus*, *Proxapertites emendates*, *Proxapertites emendates*, *Triangulorites bellus*, *Spinizonocolpites baculatus*, *Spinizonocolpites breviechinatus*, *Spinizonocolpites echinatus* with NLRs belonging to the Dipterocarpaceae, Clusiaceae, Myristicaceae, Bombacaceae, Caesalpiniaceae, Polygalaceae, Alangiaceae, Meliaceae, and Arecaceae families, all part of the evergreen vegetation of the southern Western Ghats (Prasad et al., 2009).

4.5. Climate evolution throughout the Jathang section

As regards the temperature evolution throughout the Jathang section (Fig. 11) it can be stated that in the Paleocene part, at depth level 12–14 m, temperatures were among the lowest of the present the record, then increased at depth level 15.5 m (Fig. 11). Temperature levels obtained for the profile between 17 and 20 m are characterized by very high values of the warm ends of the CA intervals (near 27 °C for CMT)

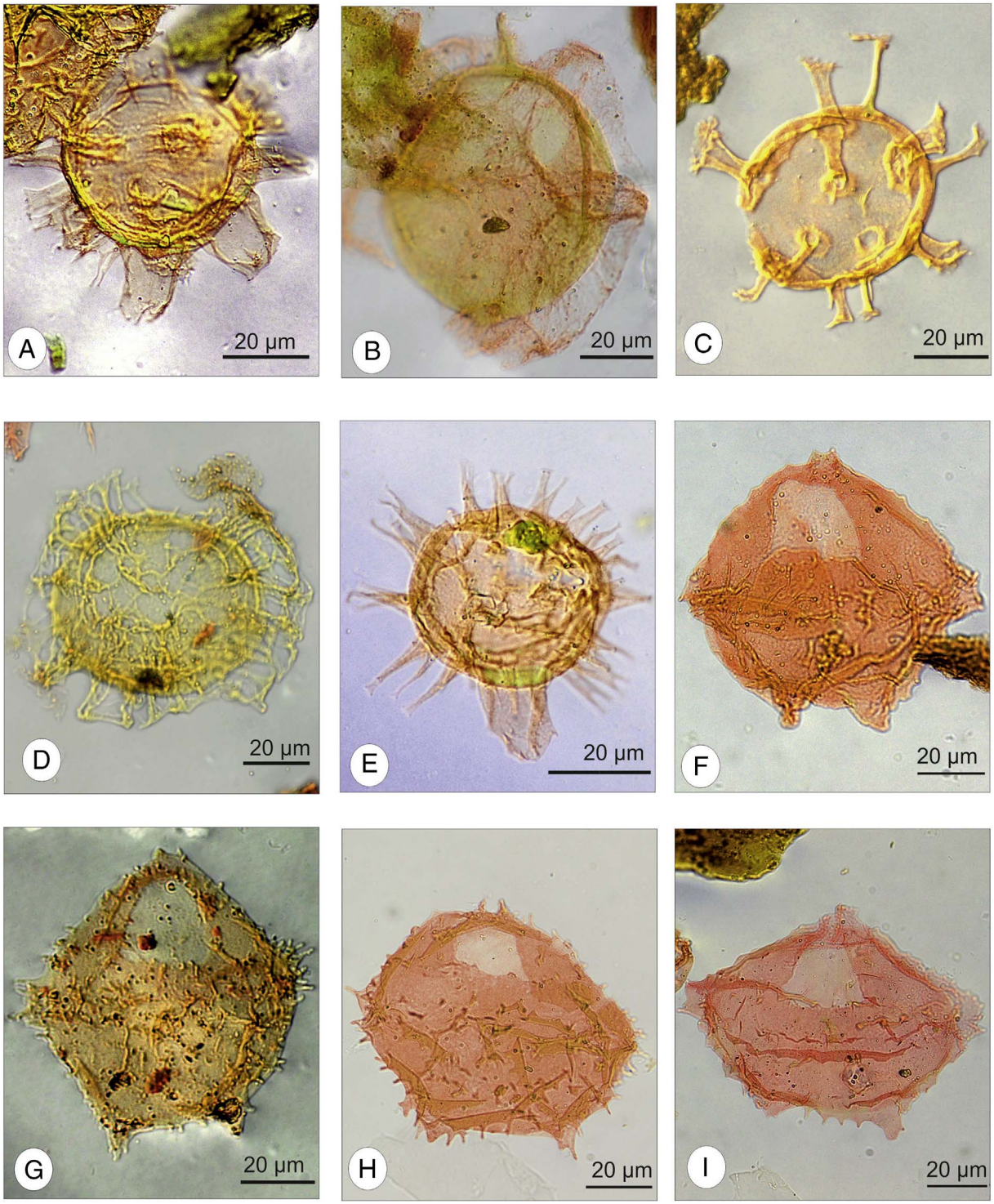

Fig. 7. Dinoflagellate cysts with slide numbers and England finder coordinates.
A, *Hystrichokolpoma rigaudiae*, BSIP 14669, P 27-3; B, *Muratodinium fimbriatum*, BSIP 14669, H 17; C, *Homotryblium tenuispinosum*, BSIP 14669, V 41; D, *Adnatospheridium multispinosum*, BSIP 14699, U 29; E, *Diphyes colligerum*, BSIP 14699, L 33; F, *Epillidinium brinkhuisii*, BSIP 14699, J 20; G, *Vallodinium picardium*, BSIP 14699, U 36; H, *Stichodinium parisiense*, BSIP 14669, L 10; I, *Epillidinium* spp., BSIP 16102, K 14.

pointing to exceptionally warm conditions with possible variability at some levels (Fig. 11). CA temperature intervals obtained for the upper part of the section, from ca. 21 m onwards, are narrower and provide a better resolution, mainly due to higher taxonomic diversity within the younger samples (Fig. 11). MAT and CMT estimates were stable and were at the same level compared to the values obtained from the samples at 20 m, while WMT was lower by ca. 2 °C (Fig. 11). Regarding changes in rainfall, MAP and MPwet display a clear trend of increasing precipitation throughout the section (Fig. 12). This trend is in accordance with the sustained decline of the number of dry days estimated from floral composition (Fig. 12). For the Paleocene part of the section, between depth levels 18–19 m, all precipitation variables have a local maximum, pointing to very wet conditions. This wet peak is succeeded by a marked decline mainly in MAP by over 300 mm and MPwet indicating drier conditions at depth level 20.3 m (Fig. 12). However, this dry episode is only constrained by a single sample for

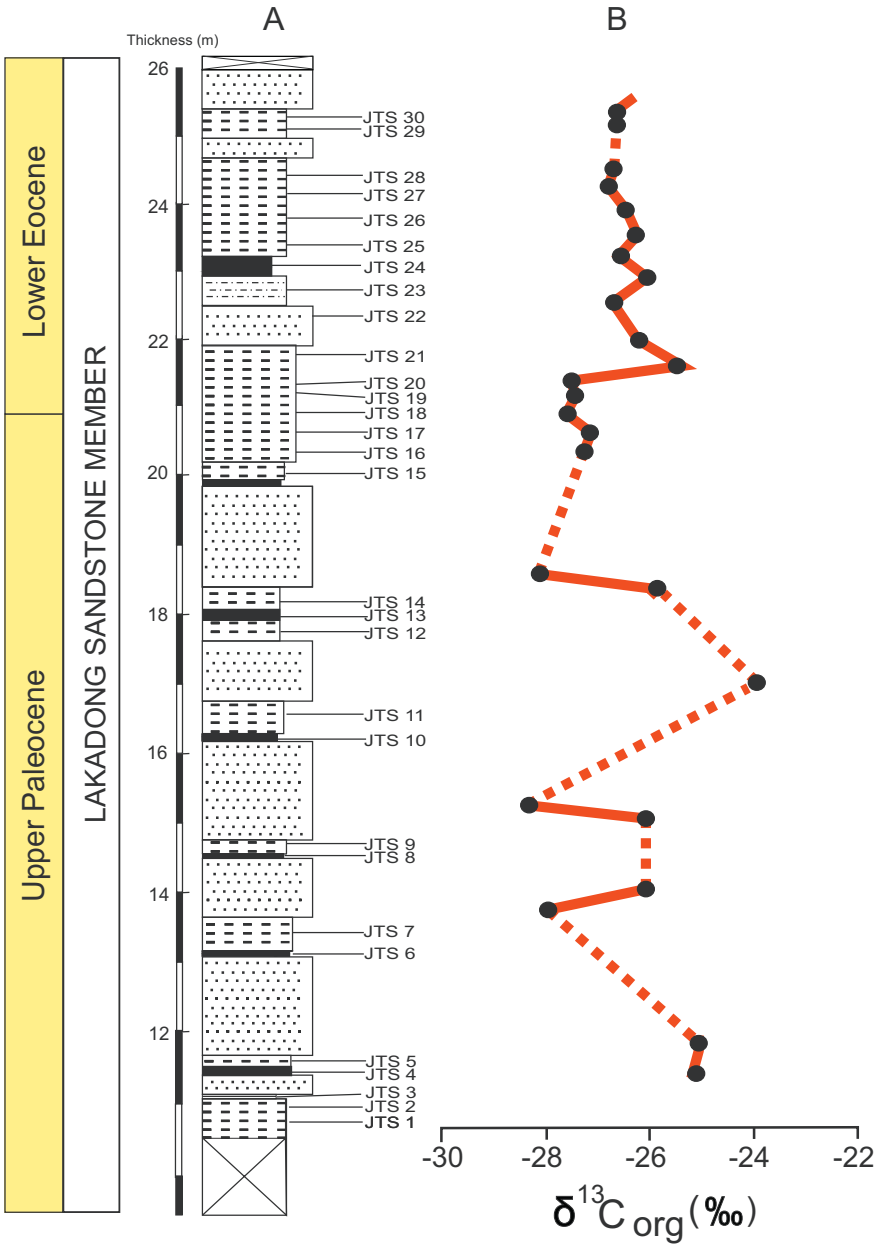

Fig. 8. Stratigraphic section at Jathang (A) and carbon isotope data (δ^{13}CTOC (‰)) (B); dotted line: sandstones (not sampled).

MAP and two samples for MPwet.

The combination of values calculated for the climatic variables indicates tropical climate (A type after Koeppen-Geiger; cf. Kottek et al., 2006), with CMT > 18 °C for all studied samples (Fig. 11). However, for the coolest parts of the Paleocene and depth level 20 m, bearing in mind large temperature intervals, a warm temperate (C type) climate cannot be excluded (CMTs < 17, 16.5 °C). To further specify an A type climate, precipitation has to be taken into account. As is obvious from the reconstructed precipitation records (Fig. 12), there is a pronounced seasonality in the rainfall signal for the entire section, being highest in the upper part of the profile, due to a very high MPwet of almost 400 mm. For the levels with MPdry from ca. 0–70 mm, mainly encountered in the lower part of the profile, conditions point to the Aw (dry winter) type according to Koeppen-Geiger, characterized by MPdry < 60 mm while higher MPdry suggested for most levels in the middle and upper part of the section point to fully humid conditions (Af type after Koeppen-Geiger).

5. Discussion

5.1. Palynofloral turnover and plant diversity

The palynoflora of Jathang indicates that two types of tropical forest, differing in floristic composition, characterized the Paleocene and early Eocene part of the section, respectively. However, this floral change was not sudden but stepwise and gradual. The low diversity Paleocene palynoflora derived from palms and pteridophytes is characteristic of lowland coastal forests, today existing in various tropical zones (Eiserhardt et al., 2011). Except for the Coryphoid palms, the majority of palms are restricted to frost-free regions of the subtropics and tropics (Tomlinson, 2006; Dransfield et al., 2008; Couvreur et al., 2011). *Borassus madagascarensis*, a coryphoid palm and NLR of the fossil pollen *Racemonocolpites* sp., is present in the Paleocene interval but completely absent during the early Eocene (Fig. 10). Similarly, *Arecipites* sp., *Liliacidites* sp., *Palmaepollenites* sp., *Palmidites* and *Monocolpites* sp., having NLRs belonging to the Arecaceae family, are characteristic

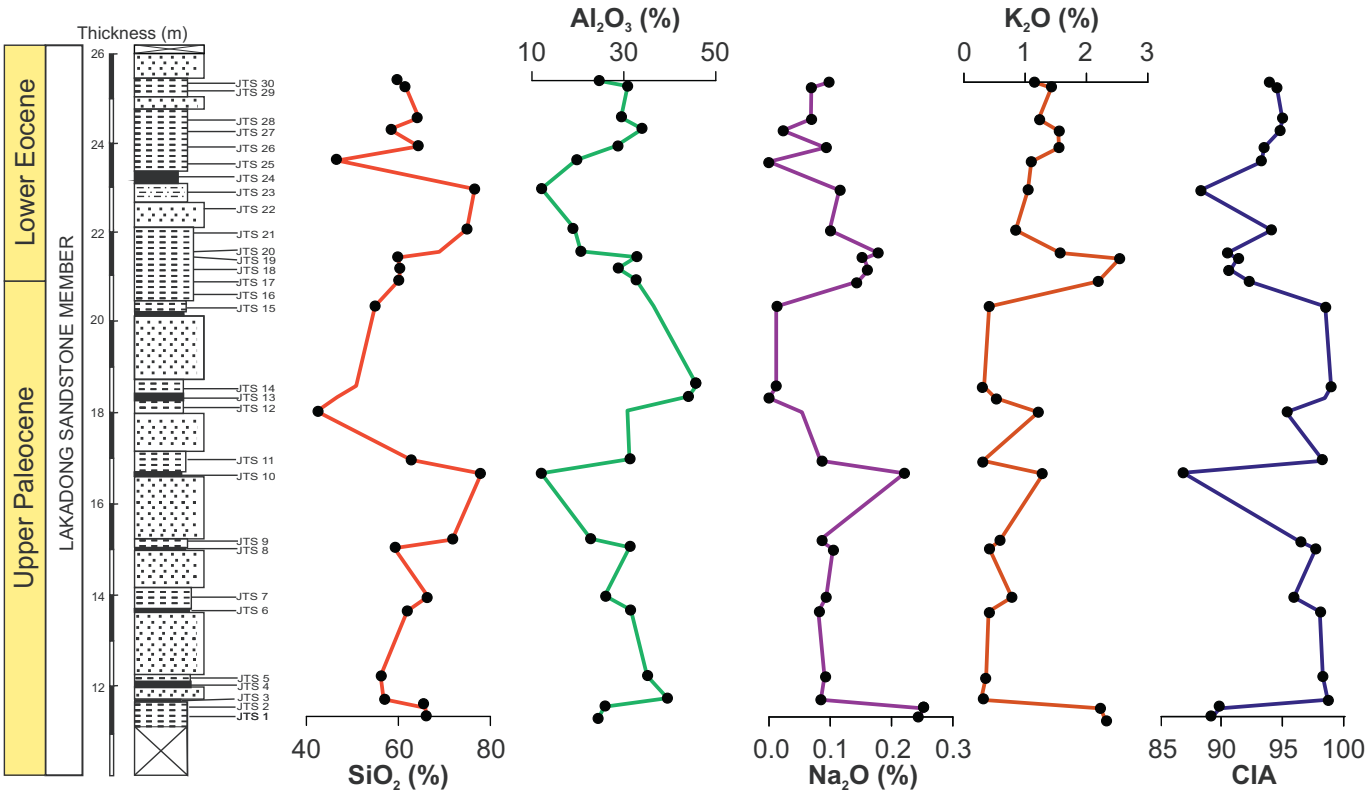

Fig. 9. Proportions of major oxides (%) and Chemical Index of Alteration (CIA).

of tropical lowland forest. They occur in the Paleocene levels (Fig. 10), but are absent from the early Eocene. A diversified dicotyledonous palyno-assemblage appeared at the Paleocene-Eocene transition. Representative genera and species of the Dipterocarpaceae, Clusiaceae, Myristicaceae, Bombacaceae, Caesalpiniaceae, Polygalaceae, Alangiceae, and Meliaceae families were introduced to the already existing Paleocene flora. Floral turnovers during the pre- and post-PETM from higher latitudinal regions, namely the Bighorn Basin, Wyoming, and North Sea realm show replacement of boreal gymnosperms by broad-leaved mesothermal and megathermal vegetation during the PETM interval, while during the recovery phase of the CIE, many typical late Paleocene-early Eocene boreal gymnosperm plants returned (Wing et al., 2005; Eldrett et al., 2014). For the low-latitude Jathang section our data indicate that the Paleocene palynoflora, characterized by low taxonomic diversity and a prevalence of palms, did not reappear in the Eocene, probably due to high precipitation and low seasonality conditions persisting in the Eocene. Similar results are also reported from the late Paleocene-early Eocene successions of Colombia and Venezuela (Jaramillo et al., 2010).

High species diversity is the characteristic feature of the equatorial rainforest. Equable climate with negligible temperature extremes and year round high precipitation are the main drivers that maintain this high diversity (Wallace, 1878; Givnish, 1999; Leigh, 1999; Leigh et al., 2004). In the present study plant standing diversity inferred from the pollen assemblages shows a significant, low diversity during the Paleocene characterized by decreased values of MAP and MPwarm as well as a longer duration of the dry season (Figs. 12, 13). Considerably higher standing plant diversity characterized the early Eocene, with a very warm, perhumid climate (Figs. 12, 13). The low diversity of the Paleocene palynoflora and highly diverse palynoflora during the early Eocene has also been observed from Paleocene-Eocene sedimentary successions of the tropical South America (Jaramillo et al., 2006; Jaramillo et al., 2010). Possibly the abrupt increase in the global CO_2 level during the PETM event at the Paleocene-Eocene transition laid the foundation of this floristic turnover. As regards the Jathang site, rapid latitudinal movements of the Indian Plate areas are as well considered as possible cause (cf. Section 5.2).

5.2. Climate reconstruction

The climate of the tropical rainforest is characterized as 'ever warm' and 'ever wet'. In reality, 'ever warm' is generally true but tropical rainforest can thrive in a wide range of rainfall intensity and seasonality (Malhi and Wright, 2004). As plant diversity involving community structure and composition is an excellent candidate for reconstructing the climate of tropical regions (Vincens et al., 2007), it has been used to explain climate change during the extreme global warm phase of the PETM from tropical South America (Jaramillo et al., 2006; Jaramillo et al., 2010).

Various studies assumed that the rise in temperature was the driving force behind the promotion of high plant diversity in the tropical biome (Jaramillo et al., 2010; Jaramillo and áCárdenas, 2013). Richness in pollen morpho-species in an angiosperm-dominated record from the Paleogene and early Neogene (65–20 Ma) of Colombia and Venezuela was found to correlate better with CO_2 rather than temperature, referred to the stimulating effect of CO_2 on productivity (Royer and Chernoff, 2013). The precipitation factor, characterized by two main aspects, namely annual mean, and month to month variability, has a major impact on tropical forest structure and hence is considered as a thrust in maintaining high biodiversity in the tropical forest biome (Barboni et al., 2003; Malhi and Wright, 2004; Vincens et al., 2007). Though palms are an integral part of most of the tropical forest vegetation (Tomlinson, 2006) continental-scale, macroecological studies indicate that precipitation seasonality is the strongest determinant of palm species richness in tropical forests (Eiserhardt et al., 2011). Hydrology also affects the composition of palm communities (Eiserhardt et al., 2011). The distribution of palm species varies between well-drained and poorly drained soils (Balslev et al., 1987). NLRs of fossil

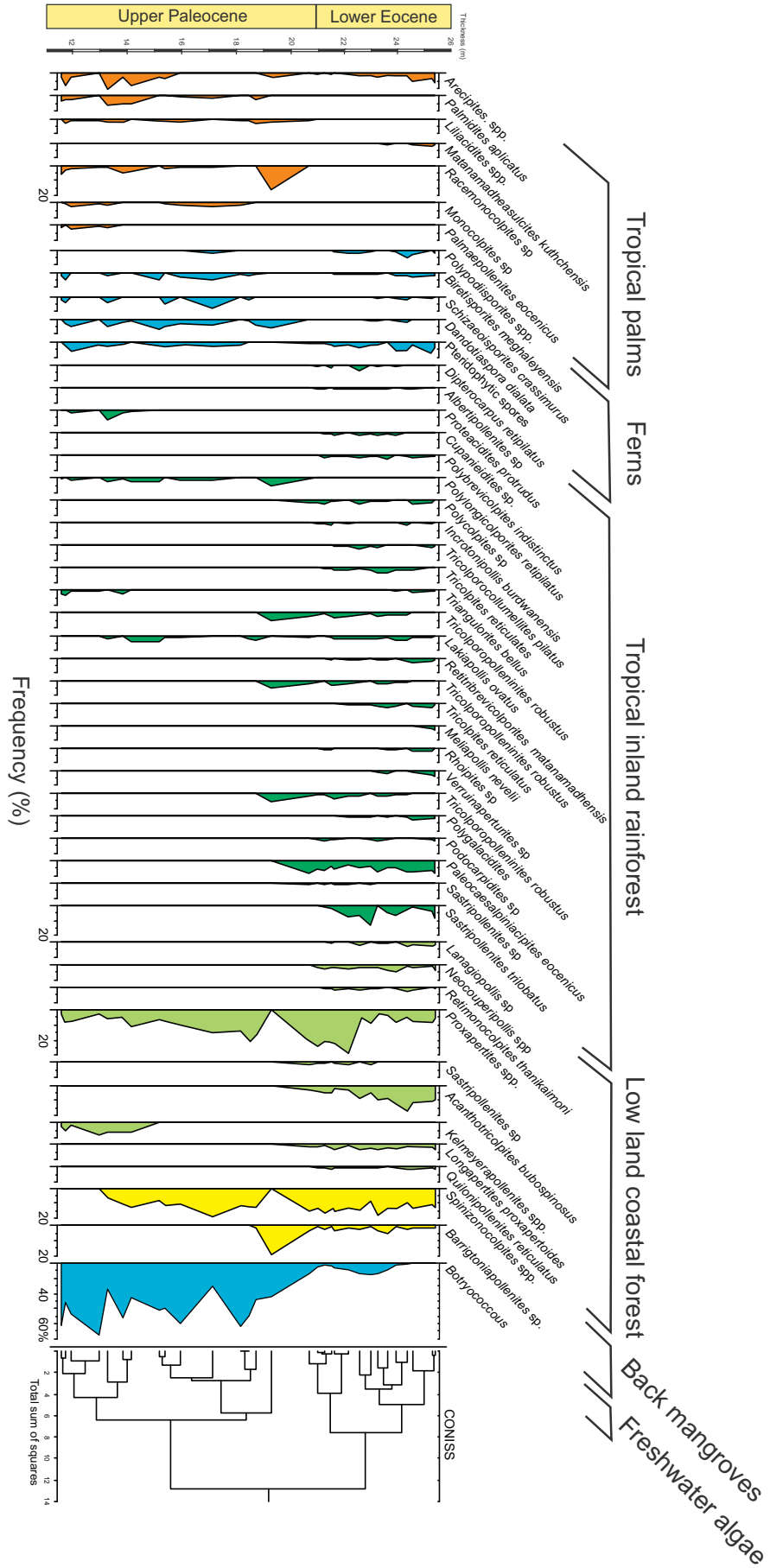

Fig. 10. Pollen and spore percentage diagram of the Jathang succession.

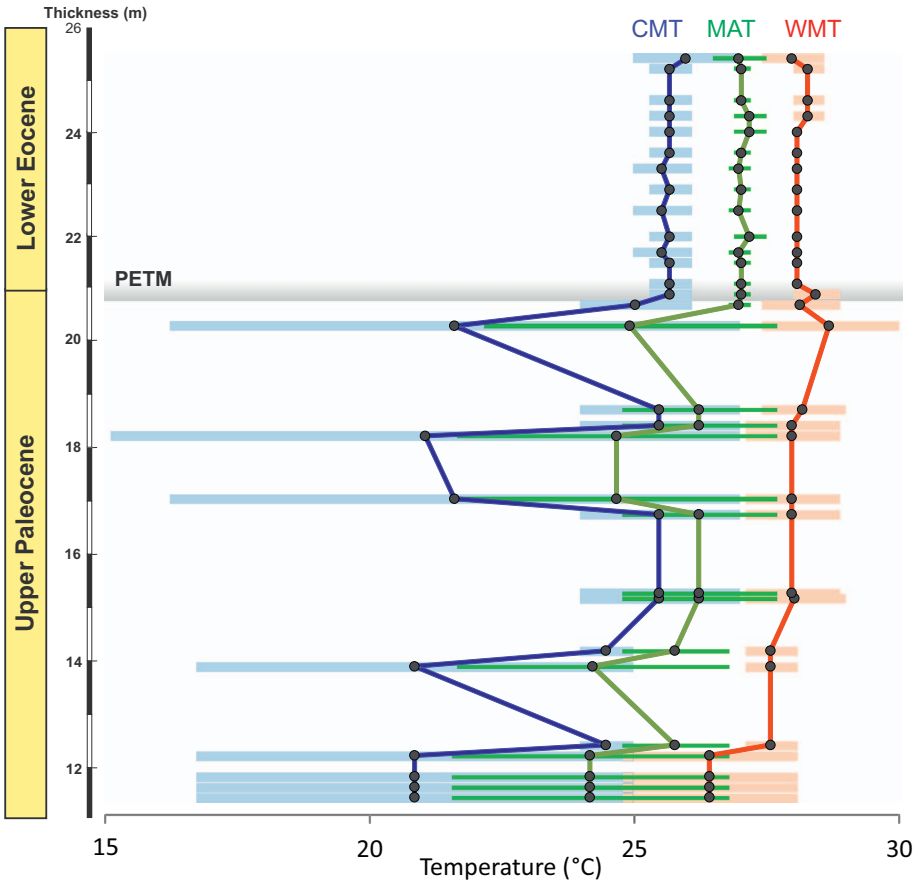

Fig. 11. Temperature records reconstructed for the Jathang succession next to profile metres (cf. Fig. 3). CMT - mean temperature of the coldest month, MAT - mean annual temperature, WMT - mean temperature of the warmest month.

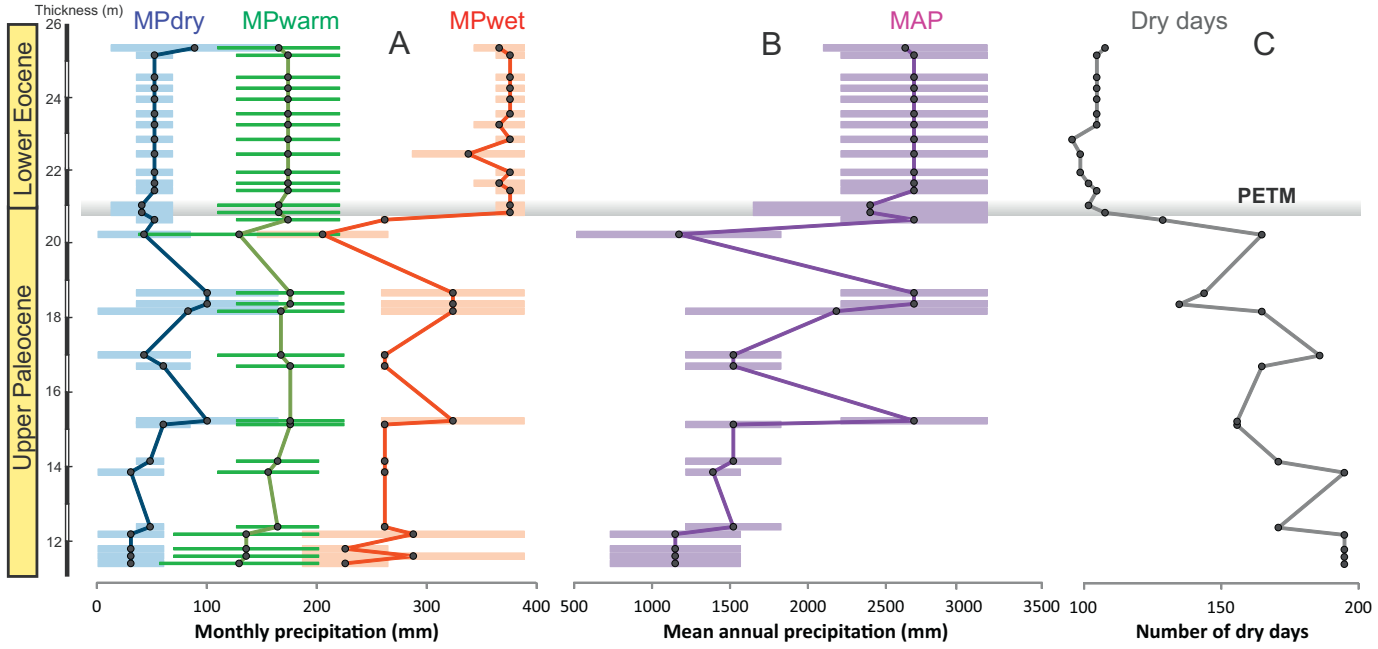

Fig. 12. Precipitation records reconstructed for the Jathang succession (A and B) and length of the dry season (C) next to profile metres (cf. Fig. 3). MPdry - mean precipitation of the driest month, MPwarm - mean precipitation of the warmest month, MPwet - mean precipitation of the wettest month, MAP - mean annual precipitation, Dry days - number of dry days.

palms present in the Paleocene part of the Jathang section have a wide MAP range and can tolerate a greater degree of fluctuations in precipitation and a distinct dry period of 5–6 months (180–150 days) (Paleoflora database). However, NLRs belonging to Nypoid palms, indicative for high MAP from ca. 1200 to 3200 mm (Paleoflora database) and a dry phase of < 3–4 months, mostly dominate in the early Eocene. The regression analysis performed in our study takes all the climatic parameters into consideration with respect to species richness

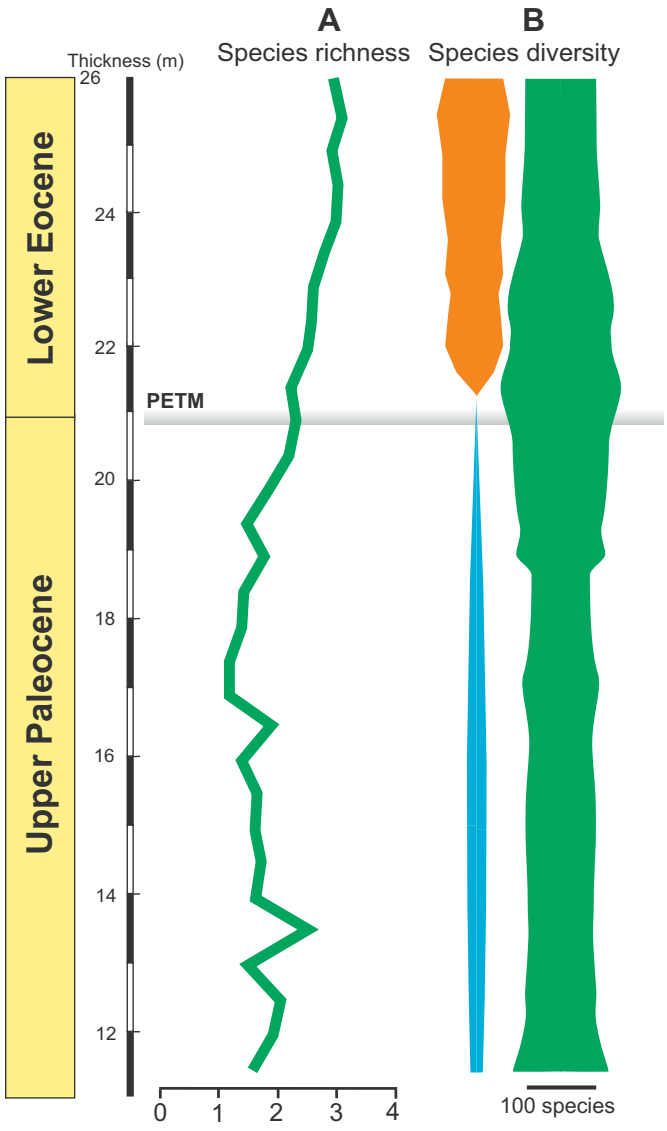

Fig. 13. Palynofloral species richness curves across the Paleocene-Eocene boundary in the Jathang section. A: the mean floral diversity per sample is significantly higher in the Eocene strata than in Paleocene strata. B: groups restricted to the Eocene (orange) and groups crossing the Paleocene-Eocene boundary (green) are more diverse than groups restricted to the Paleocene (blue). (For interpretation of the references to colour in this figure legend, the reader is referred to the web version of this article.)

(Fig. 14). The strongest negative linear correlation exists between species richness and the number of dry days ($r = 0.59$, $p < 0.001$) followed by a positive linear correlation of species richness versus wet month precipitation ($r = 0.57$, $p < 0.01$). In most cases, the correlation coefficients are significant at $p < 0.05$, except for warm month temperature, and for dry and warm month precipitation. Hence it is inferred that the number of dry days and wet month precipitation have the greatest influence on plant diversity.

When interpreting the climate records reconstructed for Jathang the rapid northward movement of the Indian Plate at that time has to be considered. When assuming a maximum age range from ca. 59–52 Ma. for the section (Thanetian to Ypresian; cf. Prasad et al., 2006) the site moved from ca. 10.4°S to 2.7°S during the deposition of the Lakadong Sandstone Member (reconstructed using GPLATES v2.00 software, hotspot frame, and plate rotations according to Matthews et al., 2016). The overall warming trend we reconstruct from the Jathang palynomorph record using the CA, evident from all accessible temperature variables (MAT, CMT, WMT) (Fig. 11), is in agreement with the climatic trend displayed by the global oxygen isotope stack (Zachos et al., 2008), showing a general warming trend throughout the later Paleocene and early Eocene that culminates in the Early Eocene Climatic Optimum at ca. 51 Ma. Moreover, the precipitation trend recorded at Jathang is in line with the drift of the plate towards lower latitudes. Sample resolution and age control in the Jathang section do not allow drawing any distinct conclusions regarding the amplitude of climate change during the PETM but point to higher temperatures at that time.

Paleolatitudes of ca. 5–3°S, as can be assumed for the Eocene part of the section, place the site in a near-equatorial position and maximum temperature levels having globally existed at that time. On the Indian subcontinent, comparable latitudes today are only reached in Sri Lanka (6°N), where MATs around 27 °C are recorded near sea-level (WorldClim dataset). The southern tip of Sumatra, located at 5.5°S is at about the same MAT level. The MAT level around 27 °C obtained for the upper part of the section indicates that early Eocene equatorial temperatures were close to the modern. However, it has to be considered that temperatures beyond the modern climate space cannot be assessed using a taxonomy-based method (Utescher et al., 2014). Thus, the assumption of significantly raised tropical temperatures during the PETM (3–5 °C; cf. Jaramillo et al., 2010) cannot be tested by using the CA. When comparing our results to other paleobotany-based climate reconstructions for the earlier Paleogene of India, our data do not support the assumption of cooler than present terrestrial temperatures in the equatorial region of India during the earlier Eocene at the continental scale as was suggested by Shukla et al. (2014) from the analysis of leaf floras in the Gurha Mine, Rajasthan, northwest India. However, more evidence for `cool´ Eocene tropics and near-tropics was obtained in other studies using multiple geochemical and plant proxies (Gulf of Mexico, equatorial Southeast Asia, Hainan Island; cf. Keating-Bitonti et al., 2011; Utescher et al., 2011; Spicer et al., 2014). These deviations may point to asymmetric continental temperature patterns and support the assumption that the low latitude Eocene climate was not uniformly warm (Spicer et al., 2014).

According to the hydrological data we have reconstructed for the Jathang section, seasonally dry climate having a dry phase of 5–6 months existed during the Paleocene, followed by considerably wetter climate conditions with a dry phase of only 2–3 months at the Paleocene-Eocene transition, persisting in the early Eocene (cf. Fig. 12, from depth level 20.5 m on). This trend towards more humid climate conditions culminating at the Paleocene-Eocene transition might be related to the general global warming trend throughout the later Paleocene to early Eocene (Zachos et al., 2008), and to raised temperatures and atmospheric CO_2 during the PETM. Our carbon isotope record (Fig. 8) shows a minor negative trend near the Paleocene-Eocene transition but does not resolve the significant excursion characteristic for the PETM. Considering this, and the lack of time control given in the section, the synchrony of these events can hardly be proven.

When taking into account the high amplitude of hydrological change reconstructed for Jathang, and the fact that the pattern changed stepwise along the section, plate tectonic movement may have played an important role. As already stated above the Indian Plate rapidly moved northward during the time-span regarded, and this might have had consequences on the prevailing precipitation regime, by far more effective than on temperature levels. Assuming a deposition time of several Myr for the Jathang succession (ca. 11 fourth-order parasequences in a shallow marine setting) and taking into account estimated paleolatitudes (see above) a northward displacement of the site in the order of 8° latitude could have moved the site from a seasonal to a perhumid tropical climate regime, depending on the paleo-position of the Inner Tropical Convergence Zone. In the Indonesian Archipelago, the transition from seasonally dry (Aw, Am of the Geiger-Koeppen system; cf. Kottek et al., 2006) to fully humid climates (Af) is found to date at ca. 7°S. This transition about coincides with the boundary between the Moist and Dry Tropical Broadleaved Forest biomes in the same region (at ca. 8°S; cf. Matthews, 1983). Thus the Jathang

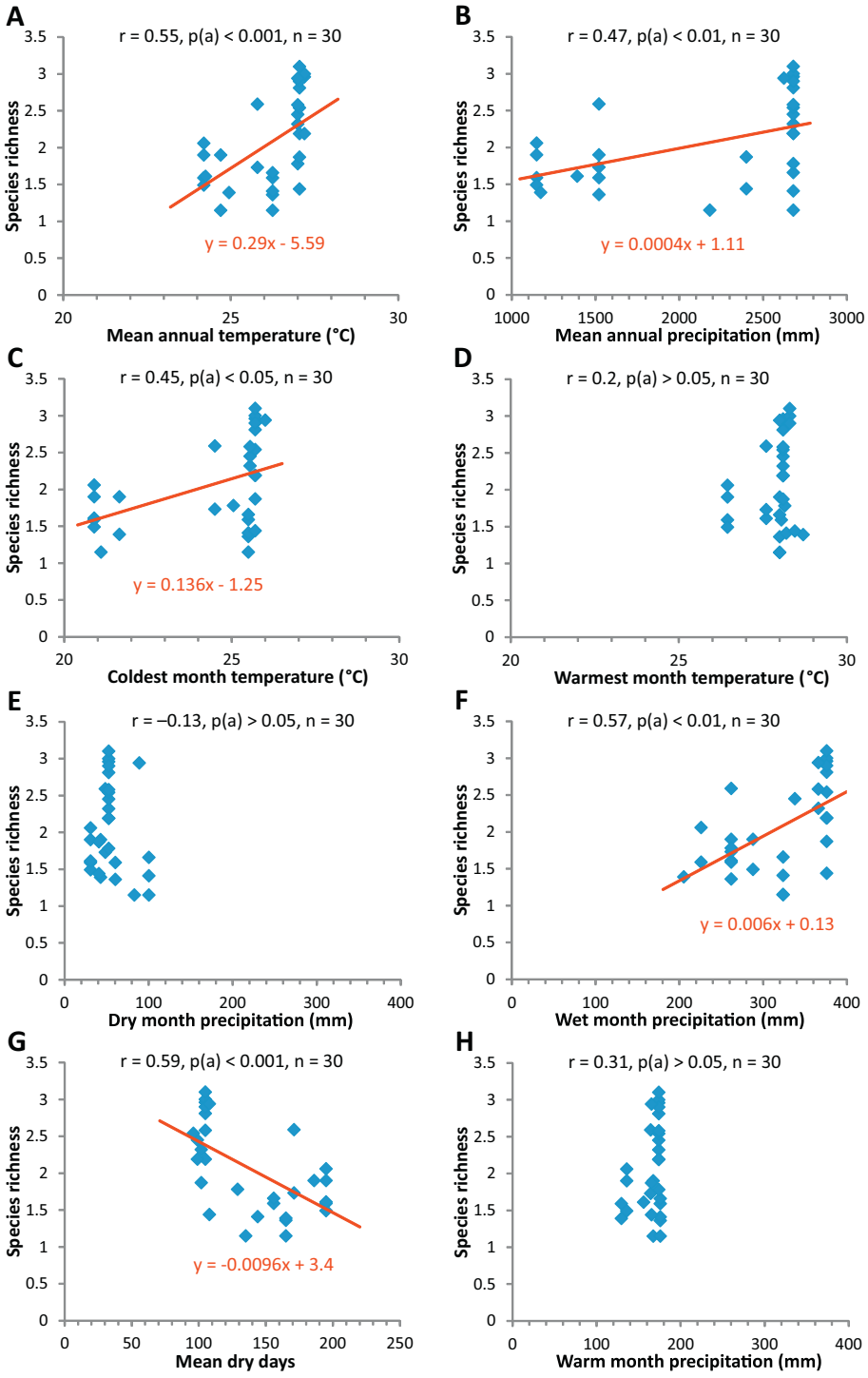

Fig. 14. Regression models for species richness versus climate data with r values. Higher r values indicate a strong linear species richness and climate variable relationship. In most cases the correlation coefficient is significant at $p < 0.05$, except for warmest month temperature (D) and driest and warmest month precipitation (E and H) ($p > 0.05$).

hydrological records are likely to represent a superimposed global and regional signal induced by plate tectonics.

The Chemical Index of Alteration (CIA) reconstructed from 26 samples of the Jathang section attains very high values > 85% (mean CIA of secondary clay minerals is ~75; cf. Nesbitt and Young, 1984) (Fig. 10) suggesting that enough water in the form of precipitation must have been available along with good drainage for flushing and a substantial residence time so that the sediment could become highly mature chemically. It is also important to note that during the deposition of the entire sequence, the conditions remained more or less consistent indicating a very warm and (seasonally) humid climate, facilitating intense weathering in the catchment.

The NLRs identified in this study are part of the tropical rainforest vegetation of the southern Western Ghats, tropical rainforests of southeast Asia (Prasad et al., 2009), rainforests of western Madagascar as well as the evergreen vegetation of Africa (Thanikaimoni et al., 1984) thus suggesting a Gondwana origin for various taxa occurring in the Paleocene-Eocene vegetation of the Indian subcontinent. The migration of megathermal plants from northeastern India to Southeast Asia took place subsequent to the Indian-Burmese plate collision.

According to Klaus et al. (2016) floristic interchange between the Indian subcontinent and mainland Asia, as estimated from the number of dispersal events, attained a maximum at ca. 50 Ma.

In this regard, paleoclimatic and floristic reconstructions for other Paleocene-Eocene successions in the paleo-equatorial belt need to be performed further to document the floral turnover and to investigate changes in plant diversity and quantify climate variability in tropical regions in a spatially explicit way.

6. Conclusions

1. Our study on a Paleocene-Eocene succession from the paleo-equatorial belt provides comprehensive palynological data allowing for a quantitative analysis of paleoclimate and plant diversity change at the Paleocene-Eocene transition.
2. Our study reveals moderately warm tropical, seasonally dry climate conditions during the Paleocene, with variable temperature and precipitation with MAT being at ca. 24–26 °C and MAP at ca. 700–1800 mm, and a dry season of 5–6 months. Particularly warm and wet, tropical climate conditions with MAT at ca. 26–27 °C and MAP at ca. 2200–3200 mm, with a considerably shorter dry season of 2–3 months, were reconstructed for the early Eocene.
3. We infer that the hydrological cycles that govern the climate of the tropics were greatly influenced by the warm climate state evolving near the Paleocene-Eocene transition and persisting throughout the early Eocene. More active hydrological cycles during this phase transformed the climate from a more variable, seasonally dry type to a more humid and equable one. The step-wise increase in precipitation observed at Jathang, combined with a successive shortening of the dry season, can be related to the fast northward movement of the Indian Plate, moving the site from a seasonal to a perhumid tropical climate regime.
4. The plant standing diversity inferred from the pollen assemblages was significantly lower under the seasonally dry tropical climate of the Paleocene. Considerably higher standing plant diversity characterizes the Paleocene-Eocene transition and the early Eocene with very warm, perhumid climate conditions. This suggests that an increase in rainfall and decrease in seasonal variability promoted the diversity of tropical plants at low latitudes during the Paleocene-Eocene transition.

Acknowledgments

VP, AS, JS, RG and PU thank the director of BSIP for providing all necessary facilities and permission to publish the manuscript (BSIP publication No 11, 2015-2016). VP and TU thank the Indian National Science Academy (Intl/CAS/2014), New Delhi, and the German Science Foundation (GZ: UT 27/2-1) for providing financial assistance. We thank our reviewers Dr. Carlos Jaramillo, Professor R. A. Spicer and an anonymous reviewer for their careful revision and helpful comments which greatly helped to improve this manuscript. This study is a contribution to the BSIP project and NECLIME (www.neclime.de). IBS is thankful to INSA Honorary Scientist position.

Appendix A. Supplementary data

Supplementary data to this article can be found online at https://doi.org/10.1016/j.palaeo.2018.02.013.

References

Allen, M.R., Ingram, W.J., 2002. Constraints on future changes in climate and the hydrologic cycle. Nature 419, 224–232.
Anupama, K., Ramesh, B.R., Bonnefille, R., 2000. The modern pollen rain from the Biligirirangan-Melagiri hills, National Seminar on Conservation of Eastern Ghats, March 24–26, 2002, held at Tirupati, Andhra Pradesh 92 of Southern Eastern Ghats, India. Rev. Paleobot. Palynol. 108 (3–4), 175–196.
Balslev, H., Luteyn, J.L., Øllgaard, B., Holm-Nielsen, L.B., 1987. Composition and structure of adjacent unflooded and floodplain forest in Amazonian Ecuador. Opera Botanica 92, 37–57.
Barboni, D., Bonnefille, R., Prasad, S., Ramesh, B., 2003. Variation in modern pollen from tropical evergreen forests and the monsoon seasonality gradient in SW India. J. Veg. Sci. 14, 551–562.
Bhandari, A., Singh, H., Rana, R.S., 2005. A note on the occurrence of Ostracoda from the Vastan Lignite Mine Gujarat. J. Palaeontol. Soc. India 50, 141–146.
Bujak, J.P., Brinkhuis, H., 1998. Global warming and dinocyst changes across the Paleocene/Eocene Epoch boundary. In: Aubry, M.P., Lucas, S.G., Berggren, W.A. (Eds.), Late Paleocene-early Eocene Climatic and Biotic Events in the Marine and Terrestrial Records. Columbia University Press, New York, pp. 277–295.
Chou, C., Neelin, J.D., 2004. Mechanisms of global warming impacts on regional tropical precipitation. J. Clim. 17, 2688–2701.
Chou, C., Neelin, J.D., Chen, C., Tu, J., 2008. Evaluating the "rich-get-richer" mechanism in tropical precipitation change under global warming. J. Clim. 22, 1982–2005.
Clark, D.A., 2004. Sources or sinks? The responses of tropical forests to current and future climate and atmospheric composition. Philos. Trans. R. Soc. Lond. B 359, 477–491.
Clementz, M., Bajpai, S., Ravikant, V., Thewissen, J.G.M., Saravanan, N., Singh, I.B., Prasad, V., 2010. Early Eocene warming events and the timing of terrestrial faunal exchange between India and Asia. Geology 39 (1), 15–18.
Cohen, J., Screen, J.A., Furtado, J.C., Barlow, M., Whittleston, D., Coumou, D., Francis, J., Dethloff, K., Entekhabi, D., Overland, J., Jones, J., 2014. Recent Arctic amplification and extreme mid-latitude weather. Nat. Geosci. 7, 627–637.
Costa, L.I., Manum, S.B., 1988. The description of the interregional zonation of Paleogene (D 1–D 15) and the Miocene (D 16–D 20). In: Vinken, Renier, Comp., The Northwest European Tertiary Basin — Results of the International Geological Correlation Programme Project No. 124. Geologisches Jahrbuch A 100, pp. 321–344.
Couvreur, T.L.P., Forest, F., Baker, W.J., 2011. Origin and global diversification patterns of tropical rainforests: inferences from a complete genus-level phylogeny of palms. BMC Biol. 9 (44 pp).
Crouch, E.M., Heilmann-Clausen, C., Brinkhuis, H., Morgans, H.E.G., Rogers, K.M., Egger, H., Schmitz, B., 2001. Global dinoflagellate event associated with the Late Paleocene Thermal Maximum. Geology 29, 315–318.
Crouch, E.M., Dickens, G.R., Brinkhuis, H., Aubry, M.-P., Hollis, C.J., Rogers, K.M., Visscher, H., 2003. The apectodinium acme and terrestrial discharge during the Paleocene-Eocene thermal maximum: new palynological, geochemical and calcareous nannoplankton observations at Tawanui, New Zealand. Palaeogeogr. Palaeoclimatol. Palaeoecol. 194, 387–403.
D'Hondt, S., Arthur, M., 1996. Late cretaceous oceans and the cool tropics paradox. Science 271, 1838–1841.
Dransfield, J., Uhl, N.W., Asmussen, C.B., Baker, W.J., Harley, M.M., Lewis, C.E., 2008. Genera Palmarum. Royal Botanic Gardens, Kew, Richmond, UK.
Dutta, S.K., Sah, S.C.D., 1970. Palynostratigraphy of the Tertiary sedimentary formations of Assam: 5 stratigraphy and palynology of South Shillong Plateau. Palaeontogr. Abt. B 131, 177–218.
Egger, H., Fenner, J., Heilmann-Clausen, C., Rögl, F., Sachsenhofer, R., Schmitz, B., 2003. Paleoproductivity of the northwestern Tethyan margin (Anthering section, Austria) across the Paleocene-Eocene transition. In: Wing, S.L., Gingerich, P.D., Schmitz, B., Thomas, E. (Eds.), Causes and Consequences of Globally Warm Climates in the Early Paleogene. Geological Society of America Special Paper 369 Geological Society of America, Boulder, Colorado, pp. 133–146.
Eiserhardt, W.L., Svenning, J.C., Kissling, W.D., Balslev, H., 2011. Geographical ecology of the palms (Arecaceae): determinants of diversity and distributions across spatial scales. Ann. Bot. 108, 1391–1416.
Eldrett, J.S., Greenwood, D.R., Polling, M., Brinkhuis, H., Sluijs, A., 2014. A seasonality trigger for carbon injection at the Paleocene-Eocene Thermal Maximum. Clim. Past 10, 759–769.
Garg, R., Khowaja-Ateequzzaman, 2000. Dinoflagellate cysts from the Lakadong Sandstone, Cherrapunji area: biostratigraphical and palaeoenvironmental significance and relavance to sea level changes in the Upper Palaeocene of the Khasi Hills, South Shillong Plateau, India. Palaeobotanist 49, 461–484.
Garg, R., Ateequzzaman, K., Prasad, V., 2006. Significant dinoflagellate cyst biohorizons in the upper cretaceous-Palaeocene succession of the Khasi Hills, Meghalaya, north east India. J. Geol. Soc. India 67, 737–747.
Garg, R., Ateequzzaman, K., Prasad, V., Tripathi, S.K.M., Singh, I.B., Jauhri, A.K., Bajpai, S., 2008. Age-diagnostic dinoflagellate cysts from the lignite-bearing sediments of the Vastan Lignite Mine Surat district Gujarat western India. J. Palaeontol. Soc. India 53, 99–105.
Givnish, T.J., 1999. On the causes of gradients in tropical tree diversity. J. Ecol. 87, 193–210.
Gogoi, B., Kalita, K.D., Garg, R., Borgohain, R., 2009. Foraminiferal biostratigraphy and palaeoenvironment of the Lakadong limestone of the Mawsynram area, south Shillong plateau, Meghalaya. J. Palaeontol. Soc. India 54 (2), 209–224.
Hammer, Ø., Harper, D.A.T., Ryan, P.D., 2001. PAST: paleontological statistics software package for education and data analysis. Palaeontol. Electron. 4 (1) (9 pp).
Haq, B.U., Hardenbol, J., Vail, P.R., 1987. Chronology of fluctuating sea levels since the Triassic. Science 235, 1156–1167.
Harding, I.C., Charles, A.J., Marshall, J.E.A., Pälike, H., Roberts, A.P., Wilson, P.A., Jarvis, E., Thorne, R., Morris, E., Moreman, R., Pearce, R., Akbari, S., 2011. Sea level and salinity fluctuations during the Palaeocene/Eocene thermal maximum in Arctic Spitsbergen. Earth Planet. Sci. Lett. 303, 97–107.
Harper, C.W., 1975. Standing diversity of fossil groups in successive intervals of geologic time: a new measure. J. Paleontol. 49, 752–757.
Huber, M., 2008. A hotter greenhouse? Science 321, 353–354.
Iakovleva, A.I., 2016. Did the PETM trigger the first important radiation of

wetzelielloideans? Evidence from France and northern Kazakhstan. Palynology 1–28. http://dx.doi.org/10.1080/01916122.2016.1173121.
IPCC, 2007. Climate change: the physical science basis. In: Solomon, S., Qin, D., Manning, M., Chen, Z., Marquis, M., Averyt, K.B., Tignor, M., Miller, H.L. (Eds.), Contribution of Working Group I to the Fourth Assessment Report of the Intergovernmental Panel on Climate Change. Cambridge University Press, Cambridge, UK.
Jaramillo, C., áCárdenas, A., 2013. Global warming and neotropical rainforests: a historical perspective. Annu. Rev. Earth Planet. Sci. 41, 741–766.
Jaramillo, C.A., Rueda, M.J., Mora, G., 2006. Cenozoic plant diversity in the Neotropics. Science 311, 1893–1896.
Jaramillo, C., Ochoa, D., Contreras, L., et al., 2010. Effects of rapid global warming at the Paleocene-Eocene boundary on Neotropical vegetation. Science 330, 957–961.
Jauhri, A.K., Agarwal, K.K., 2001. Early Palaeogene in the south Shillong Plateau, NE India: local biostratigraphic signals of global tectonic and oceanic changes. Palaeogeogr. Palaeoclimatol. Palaeoecol. 168, 187–203.
Kar, R.K., Kumar, M., 1986. Palaeocene palynostratigraphy of Meghalaya, India. Pollen Spores 28, 177–218.
Keating-Bitonti, C.R., Ivany, L.C., Affek, H.P., Douglas, P., Samson, S.D., 2011. Warm, not super-hot, temperatures in the early Eocene subtropics. Geology 39, 771–774.
Kender, S., Stephenson, M.H., Riding, J.B., Leng, M.J., Knox, R.W.O.B., Peck, V.L., Kendrick, C.P., Ellis, M.A., Vane, C.H., Jamieson, R., 2012. Marine and terrestrial environmental changes in NW Europe preceding the carbon release at the Paleocene-Eocene transition. Earth Planet. Sci. Lett. 353–354, 108–120.
Klaus, S., Morely, R.J., Plath, M., Zhang, Y.-P., Li, J.-T., 2016. Biotic interchange between the Indian subcontinent and mainland Asia through time. Nat. Commun. 7, 12132. http://dx.doi.org/10.1038/ncomms12132.
Kottek, M., Grieser, J., Beck, C., Rudolf, B., Rubel, F., 2006. World map of the Köppen-Geiger climate classification ogischeeitschriftupdated. Meteorol. Z. 15, 259–263.
Kumar, M., Spicer, R.A., Spicer, T.E.V., Shukla, A., Mehrotra, R.C., Mong, P., 2016. Palynostratigraphy and palynofacies of the early Eocene Gurha lignite mine, Rajasthan, India. Palaeogeogr. Palaeoclimatol. Palaeoecol. 461, 98–108.
Leigh, E.G., 1999. Tropical Forest Ecology. A View From Barro Colorado Island. Oxford Univ. Press, New York, Oxford (245pp).
Leigh Jr., E.G., Davidar, P., Dick, C.W., Puyravaud, J.-P., Terborgh, J., TerSteege, H., Wright, S.J., 2004. Why do some tropical forests have so many species of trees? Biotropica 36, 447–473.
Malhi, Y., Wright, J., 2004. Spatial patterns and recent trends in the climate of tropical rainforest regions. Philos. Trans. R. Soc. Lond. B 359, 311–329.
Masson-Delmotte, V., Kageyama, M., Braconnot, P., Charbit, S., Krinner, G., Ritz, C., Guilyardi, E., Jouzel, J., Abe-Ouchi, A., Crucifix, M., Gladstone, R.M., Hewitt, C.D., Kitoh, A., LeGrande, N., Marti, O., Merkel, U., Motoi, T., Ohgaito, R., Otto-Bliesner, B., Peltier, W.R., Ross, L., Valdes, P.J., Vettoretti, G., Weber, S.L., Wolk, F., Yu, Y., 2006. Past and future polar amplification of climate change: climate model intercomparisons and ice-core constraints. Clim. Dyn. 26, 513–529.
Matthews, E., 1983. Global vegetation and land use: new high-resolution data bases for climate studies. J. Clim. Appl. Meteorol. 22, 474–487.
Matthews, K.J., Maloney, K.T., Zahirovic, S., Williams, S.E., Seton, M., Müller, R.D., 2016. Global plate boundary evolution and kinematics since the late Paleozoic. Glob. Planet. Chang. http://dx.doi.org/10.1016/j.gloplacha.2016.10.002.
Meehl, G.A., Collins, W.D., Boville, B.A., Kiehl, J.T., Wigley, T.M.L., Arblaster, J.M., 2000. Response of the NCAR climate system model to increased CO_2 and the role of physical processes. J. Clim. 13, 1879–1898.
Mosbrugger, V., Utescher, T., 1997. The coexistence approach – a method for quantitative reconstructions of Tertiary terrestrial palaeoclimate data using plant fossils. Palaeogeogr. Palaeoclimatol. Palaeoecol. 134, 61–86.
Nagappa, Y., 1959. Foraminiferal biostratigraphy of Cretaceous-Eocene succession in the India-Pakistan-Burma region. Micropaleontology 5, 145–192.
Nesbitt, H.W., Young, G.M., 1984. Prediction of some weathering trends of plutonic and volcanic rocks based on thermodynamic and kinetic considerations. Geochim. Cosmochim. Acta 54, 1523–1534.
Pascal, J.P., Pélissier, R., 1996. Structure and floristic composition of a tropical evergreen forest in south-west India. J. Trop. Ecol. 12, 195–218.
Powell, A.J., 1992. Dinoflagellate cysts of the tertiary system. In: Powell, A.J. (Ed.), A Stratigraphic Index of Dinoflagellate Cysts. Chapman and Hall, London, pp. 155–252.
Prasad, V., Garg, R., Khowaja-Ateequzzaman, Singh, I.B., Joachimski, M., 2006. Apectodinium acme and the palynofacies characteristics in the latest Palaeocene–earliest Eocene of north eastern India: biotic response to Palaeocene–Eocene Thermal Maxima (PETM) in low latitude. J. Palaeontol. Soc. India 51, 75–91.
Prasad, V., Farooqui, A., Tripathi, S.K.M., Garg, R., Thakur, B., 2009. Evidence of Late Palaeocene–Early Eocene equatorial rain forest refugia in southern Western Ghats India. J. Biosci. 34, 777–797.
Prasad, V., Singh, I.B., Bajpai, S., Garg, R., Thakur, B., Singh, A., Saravanan, N., Kapur, V.V., 2013. Palynofacies and sedimentology-based high-resolution sequence stratigraphy of the lignite-bearing muddy coastal deposits (early Eocene) in the Vastan Lignite Mine, Gulf of Cambay, India. Facies 59, 737–761.
Raja Rao, C.S., 1981. Coalfields of India: coalfields of northeastern India. Bull. Geol. Surv. India Ser. A 45, 1–76.
Ramesh, B.R., Pascal, J.P., 1997. Atlas of Endemics of the Western Ghats (India). Distribution of Tree Species in the Evergreen and Semi-evergreen Forest. French Institute of Pondicherry, Pondicherry, India.
Rose, K.D., Smith, T., Rana, R.S., Sahni, A., Singh, H., Missiaen, P., Folie, A., 2006. Early Eocene (Ypresian) continental vertebrate assemblage from India, with description of a new anthracobunid (Mammalia, Teththeria). J. Vertebr. Paleontol. 26, 219–225.
Royer, D.L., Chernoff, B., 2013. Diversity in neotropical wet forests during the Cenozoic linked more to atmospheric CO_2 than temperature. Proc. R. Soc. B 280, 22013–22024.
Sahni, A., Rana, R.S., Loyal, R.S., Saraswati, P.K., Mathur, S.K., Tripathi, S.K.M., Rose, K.D., Garg, R., 2004. Western Margin Palaeocene-lower Eocene Lignites: Biostratigraphic and Palaeoecological Constraints: 2nd Association of Petroleum Geologists coNference and Exhibition. Khajuraho. pp. 1–18.
Sahni, A., Saraswati, P.K., Rana, R.S., Kumar, K., Singh, H., Alimohammadian, H., Sahni, N., Rose, K.D., Singh, L., Smith, T., 2006. Temporal constraints and depositional paleoenvironments of the Vastan Lignite sequence Gujarat: analogy for the Cambay Shale hydrocarbon source rock. Indian J. Petrol. Geol. 15, 1–20.
Saini, N.K., Mukherjee, P.K., Rathi, M.S., Khanna, P.P., 2000. Evaluation of energy dispersive X-ray fluorescence spectrometry in the analysis of silicate rocks using pressed powder pellets. X-Ray Spectrom. 29, 166–172.
Samant, B., Phadtre, N.R., 1997. Stratigraphic palynoflora of the early Eocene Rajpardi lignite, Gujarat and the lower age limit of the Tarkeshwar Formation of South Cambay Basin, India. Palaeontogr. Abt. B 245, 1–108.
Scotese, C.P., Golanka, J., 1992. Paleogeographic Atlas, PALEOMAP Progress Rep. 20-0692 (34 pp.). Univ. of Tex. at Arlington, Arlington.
Shukla, A., Mehrotra, R.C., Spicer, R.A., Spicer, T.E.V., Kumar, M., 2014. Cool equatorial terrestrial temperatures and the South Asian monsoon in the Early Eocene: evidence from the Gurha Mine, Rajasthan, India. Palaeogeogr. Palaeoclimatol. Palaeoecol. 412, 187–198.
Singh, I.B., Swamy, A.S.R., 2006. Delta Sedimentation: East Coast of India. Technology publication (392 pp).
Sluijs, A., Brinkhuis, H., Crouch, E.M., John, C.M., Handley, L., Munsterman, D., Bohaty, S.M., Zachos, J.C., Reichart, G.-J., Schouten, S., Pancost, R.D., Sinni, J.S., Welters, N.L.D., Lotter, A.F., Dickens, G.R., 2008. Eustatic variations during the Paleocene-Eocene greenhouse world. Palaeoceanography 23, PA4216. http://dx.doi.org/10.1029/2008PA001615.
Spicer, R.A., Herman, A.B., Liao, W., Spicer, T.E.V., Kodrul, T.M., Yang, J., Jin, J., 2014. Cool tropics in the Middle Eocene: Evidence from the Changchang Flora, Hainan Island, China. Palaeogeogr. Palaeoclimatol. Palaeoecol. 412, 1–16.
Srivastava, J., Prasad, V., 2015. Effect of global warming on diversity pattern in Nypa mangroves across Paleocene-Eocene transition in the paleo-equatorial region of the Indian sub-continent. Palaeogeogr. Palaeoclimatol. Palaeoecol. 429, 1–12.
Stork, A.L., Smith, D.K., Gill, J.B., 1987. Evaluation of geochemical reference standards by X-ray fluorescence analysis. Geostand. Newslett. 11, 107–113.
Thanikaimoni, G., Caratini, C., Venkatachala, B.S., Ramanujam, C.G.K., Kar, R.K., 1984. Selected Tertiary angiosperm pollen from India and their relationship with African Tertiary pollen. In: Travaux de la Section Scientifique et Technique 19. Institut Français de Pondichéry, pp. 1–93.
Tissot, C., Chikhi, H., Nayar, T.S., 1994. Pollen of Wet Evergreen Forests of the Western Ghats India, Inst. Fr. Pondichery 35. pp. 133.
Tomlinson, P.B., 2006. The uniqueness of palms. Bot. J. Linn. Soc. 151, 5–14.
Tripathi, S.K.M., Saxena, R.K., Prasad, V., 2000. Palynological investigation of the Tura Formation (early Eocene) exposed along the Tura-Dalu Road, west Garo Hills, Meghalaya, India. Palaeobotanist 49, 239–251.
Utescher, T., Mosbrugger, V., 2014. The Palaeoflora Database. www.palaeoflora.de.
Utescher, T., Bruch, A.A., Micheels, A., Mosbrugger, V., Popova, S., 2011. Cenozoic climate gradients in Eurasia a palaeo-perspective on future climate change? Palaeogeogr. Palaeoclimatol. Palaeoecol. 304, 351–358.
Utescher, T., Bruch, A.A., Erdei, B., François, L., Ivanov, D., Jacques, F.M.B., Kern, A.K., Liu, Y.-S.C., Mosbrugger, V., Spicer, R.A., 2014. The coexistence approach—theoretical background and practical considerations of using plant fossils for climate quantification. Palaeogeogr. Palaeoclimatol. Palaeoecol. 410, 58–73.
Vincens, A., Garcin, Y., Buchet, G., 2007. Influence of rainfall seasonality on African lowland vegetation during the Late Quaternary: pollen evidence from Lake Masoko, Tanzania. J. Biogeogr. 34, 1274–1288.
Wallace, A.R., 1878. Tropical Nature and Other Essays. Macmillan, London.
Williams, G.L., Damassa, S.P., Fensome, R.A., Guerstein, R.G., 2015. Wetzeliella and its allies – the 'hole' story: a taxonomic revision of the Paleogene dinoflagellate subfamily Wetzelielloideae. Palynology. http://dx.doi.org/10.1080/01916122.2014.993888.
Wilson, G.F., Metre, W.B., 1953. Assam and Arakan. In: Illing, V.C. (Ed.), The World's Oil Fields: The Eastern Hemisphere. The Science of Petroleum 6(1). Published by Oxford Univ. Press, pp. 119–123.
Wing, S.L., Harrington, G.J., Smith, F.A., Bloch, J.I., Boyer, D.M., Freeman, K.H., 2005. Transient floral change and rapid global warming at the Paleocene-Eocene boundary. Science 310, 993–996.
Zachos, J.C., Dickens, G.R., Zeebe, R.E., 2008. An early Cenozoic perspective on greenhouse warming and carbon-cycle dynamics. Nature 451, 279–283.